

Repurposing ubiquitination for innovative antibody conjugation

Hebieshy, A.F. el

Citation

Hebieshy, A. F. el. (2025, October 16). *Repurposing ubiquitination for innovative antibody conjugation*. Retrieved from https://hdl.handle.net/1887/4273517

Version: Publisher's Version

Licence agreement concerning inclusion of doctoral

License: thesis in the Institutional Repository of the University

of Leiden

Downloaded from: https://hdl.handle.net/1887/4273517

Note: To cite this publication please use the final published version (if applicable).





Ubiquitin as a conjugation tag for labeling and multimerization of antibodies

2

This chapter is part of the publication:

A.F. Elhebieshy*, Z. Wijfjes*, et al. Site-directed multivalent conjugation of antibodies to ubiquitinated payloads. Accepted for publication: Nature Biomedical Engineering.



Ubiquitin as a conjugation tag for labeling and multimerization of antibodies

Angela F. el Hebieshy, Johan M. S. van Der Schoot, Jim Middelburg, Marjolein Sluijter, Thorbald van Hall, Douwe J. Dijkstra, Leendert A. Trouw, Cami M. P. Talavera Ormeño, Bjorn R. van Doodewaerd, Paul W. H. I. Parren, Gerbrand J. van der Heden van Noort, Martijn Verdoes, Ferenc A. Scheeren, Huib Ovaa.

Abstract

Antibody conjugates form a foundation for many research-, diagnostic-, and therapeutic applications. Despite the robustness and efficiency of existing antibody conjugation techniques, the challenge of efficiently obtaining homogeneous products remains. Here, we developed a versatile modular method for site-directed antibody conjugation using the small protein ubiquitin. We show that ubiquitin, when fused to antibodies or antibody fragments, is conjugated using in vitro ubiquitin ligation with an average efficiency of 94%. We effectively applied this method, which we named ubi-tagging, to conjugate chemically synthesized ubiquitin with a site-specifically incorporated payload (fluorophore) to ubi-tagged Fab fragments. Additionally, we show that this method can be efficiently used to generate di-, tri-, and multi-valent antibody complexes and to generate a bi-specific T cell activator. The combined use of both recombinant ubitags and synthetic ubiquitin allows homogeneous site-directed antibody conjugation with defined conjugates incorporating precise functionalities while retaining antibody functionality.

Introduction

Antibodies are indispensable tools in the fields of chemical biology, diagnostics and therapeutics, owing to their high selectivity and affinity towards specific target molecules.

Over the past decade, the interest in antibody-based reagents and therapeutics of higher complexity than monoclonal antibodies has been growing steeply. This led to the soaring development of antibody engineering technologies for the production of antibody conjugates and multivalent antibody formats such as antibodies conjugated to fluorophores for analytical or diagnostic applications, antibodies conjugated to small molecules forming antibody-drug conjugates (ADCs), and bi- or multi-specific antibodies targeting multiple targets simultaneously.

Conventional antibody conjugation strategies rely on the random attachment to certain amino acid residues along the antibody. These techniques make use of the chemical properties of the side chain of lysine or cysteine residues through NHS labeling or thiol-reactive maleimide groups, respectively^{1–3}. Despite being used in clinical-grade antibody products, such random modifications result in highly heterogeneous products,

with limited control over the number and site of modifications, often compromising antibody functionality and pharmacokinetics⁴⁻⁷. Remarkable advances have been made in developing site-specific conjugation techniques to overcome these challenges, including the incorporation of non-natural amino acids in the antibody sequence carrying reactive groups for bio-orthogonal chemistry 8-12, glycan-remodeling of native glycans to install an unnatural sugar containing a conjugation handle¹³⁻¹⁵, and the fusion of a peptide tag to the antibody that can be specifically modified enzymatically. Well-exemplified in the latter category are ligation strategies based on enzymes such as transglutaminase, formylglycine-generating enzyme (FGE), and sortase. Microbial transglutaminase (mTG) recognizes a specific glutamine-containing sequence and covalently attaches an amine-functionalized linker carrying a payload or conjugation handle to the glutamine residue while expelling ammonia^{5,16}. Formylglycine-generating enzyme (FGE) converts the cysteine residue present in its recognition motif to an aldehyde functional group which serves as a conjugation handle 17,18, while sortase mediates the ligation of its recognition sequence to an oligoglycine peptide attached to a payload, peptide or conjugation handle 19-22. These techniques are site-specific and modular for the ligation of synthetic payloads to antibodies or antibody fragments, however, significant challenges remain. In particular, long reaction times on the order of hours and even days, limited reaction efficiency, and poor yields are key limitations to using these techniques^{5,17,21–23}. Additionally, a two-step approach is required when using these techniques for protein-protein conjugation, for example to generate a bispecific antibody^{23,24}, which is time consuming and often leads to reduced yields.

To address these limitations, here we introduce a novel versatile modular approach for site-specific antibody conjugation based on ubiquitin biochemistry and the chemical synthesis of ubiquitin-related tools. We set out to determine the use of ubiquitin as a conjugation tag for the site-selective attachment of different moieties to antibodies and the generation of multivalent antibody complexes in a controlled manner using ubiquitinating enzymes (Fig. 1a).

Ubiquitin (Ub) is a small protein tag involved in almost all cellular processes^{25–28}. It is a 76-amino acid post-translational modifier that is covalently attached to target proteins in a highly regulated process called ubiquitination. This process is coordinated by an enzymatic cascade involving ubiquitin-activating (E1)²⁹, ubiquitin-conjugating (E2)³⁰, and ubiquitin-ligating (E3)^{31,32} enzymes, resulting in the covalent attachment of the C-terminal glycine residue of ubiquitin to the N-terminus or lysine residues of target proteins. Ubiquitin molecules also have the ability to be conjugated to each other at one of the seven internal lysine residues or at the N-terminal methionine residue. This results in the formation of ubiquitin chains with different linkage types²⁶. Notably, the linkage type involved in ubiquitin chain-formation is regulated by different E2 and E3 enzymes^{31–34}. Linkage-specific ubiquitin chains of all types can therefore be efficiently

ligated *in vitro* using the appropriate recombinant E1, E2, and E3 enzymes³⁵. The E2 and E3 can be provided as a fusion protein³⁶ to increase ligation activity (Fig. 1a). In addition, using specific ubiquitin mutants, the process of ubiquitin chain formation can be fully controlled^{35,37}. These features combined make the exploitation of ubiquitin and the ubiquitination machinery an interesting approach to selectively generate antibody conjugates that are site-specifically joined through ubiquitin chains of a specific ubiquitin-linkage type. Fusing ubiquitin to an antibody at a position not affecting its binding, hereafter referred to as ubi-tagging, would allow the precise *in vitro* engineering of this ubiquitin at specific lysine residues depending on the E2 and E3 used. Ubi-tagged antibodies can be conjugated to another ubiquitin fused-antibody, making a bispecific antibody, or to a chemically synthesized ubiquitin carrying selected modifications such as a fluorophore, label, or cytotoxic drug. This provides a modular platform for the generation of ubiquitin-based antibody conjugates of limitless different architectures, marrying the advantages of (therapeutic) protein engineering and synthetic chemistry.

The vast potential of ubi-tagging is exemplified by the generation of homogeneous conjugates, including fluorescently-labeled Fab fragments and defined Fab multimers. Moreover, we demonstrate ubiquitin chain elongation of Fab hetero-dimers to form hetero-trimers and show that ubi-tagged conjugates can be site-specifically cleaved using deubiquitinating enzymes.

Results

Generation and characterization of ubi-tagged antibody fragments

As a proof of principle, we selected monovalent Fab fragments to characterize ubiquitin conjugation in the context of antibody-ubiquitin fusion. The Fab fragment is produced as a fusion protein with a ubi-tag followed by a His-tag at the C-terminus of its heavy chain (Fig. 1b). We generated recombinant ubi-tagged Fab fragments using CRISPR/HDR, which we recently developed for the production of modified recombinant antibodies³⁸. The IgH locus of parental hybridoma cell line anti-CD3 (KT3, mlgG2a) WT was genetically modified to switch production from WT mAbs to ubiquitin-His-tagged Fabs (Fig. 1c). The genetically-modified monoclonal cell lines were assessed for the secretion of Ubiquitin-His-tagged Fab fragments using an anti-his secondary antibody. The supernatant of over 80% of the single-cell colonies that grew out after antibiotic selection were positive for the His-tag, indicating that these edited monoclonal cell lines produced a ubi-tagged Fab fragment (Fig. 1d). Next, we selected a monoclonal cell line highly expressing the ubi-tagged Fab and expanded it for further characterization. The Fab fragments isolated from the supernatants were validated for the presence of the ubi-tag on the heavy chain by resolving on SDS-PAGE, with or without prior reduction using β-mercaptoethanol, followed by anti-ubiquitin western blotting (Fig. 1e).

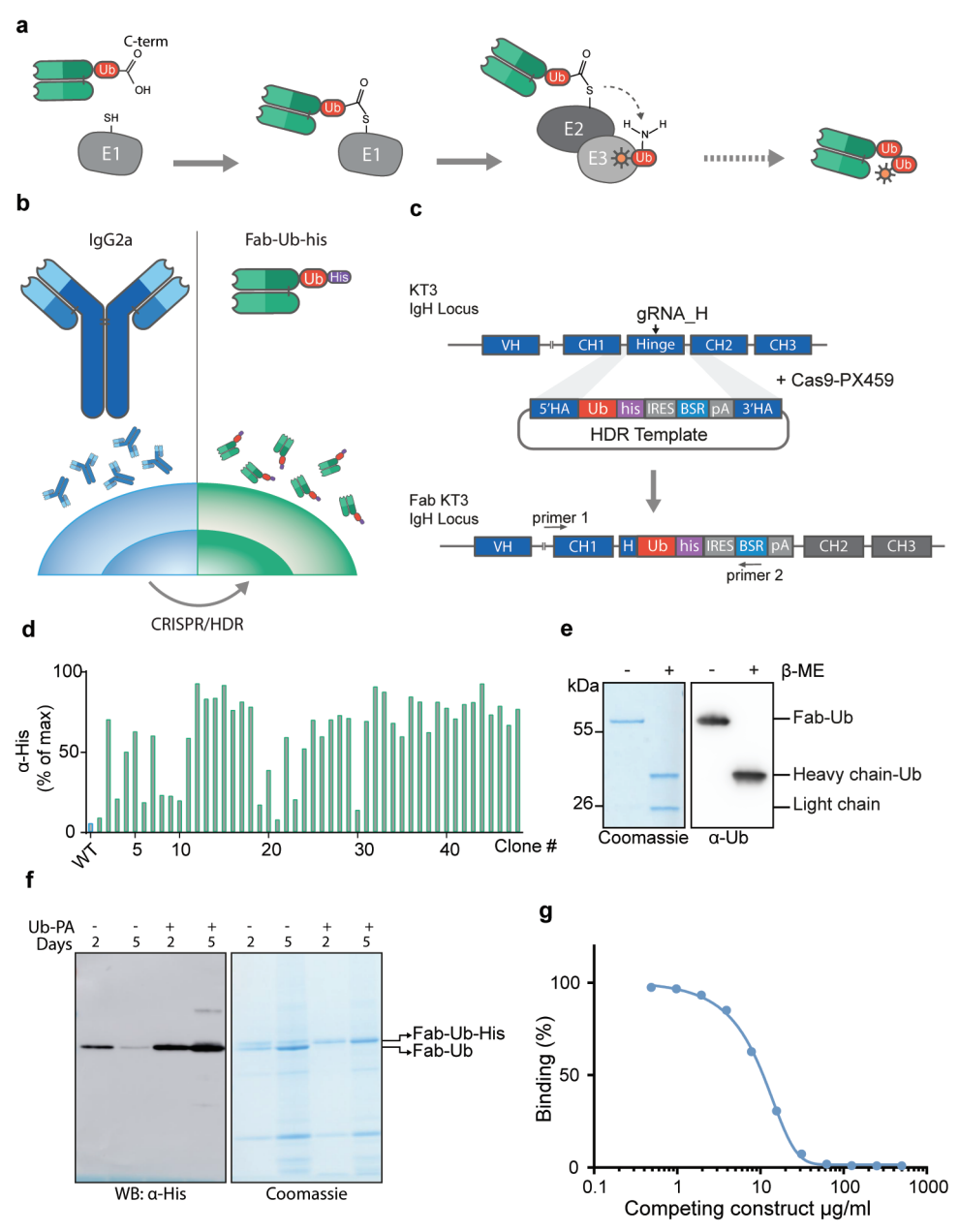


Figure 1| Generation and site-specific labeling of ubi-tagged antibody fragments. (a) Schematic illustration of ubi-tag conjugation using the ubiquitination cascade. The ubi-tag C-terminus is activated by the E1 enzyme to form a thioester bond. The activated ubi-tag is then transferred to an E2 enzyme which then, with the help of an E3 enzyme, specifically transfers it to a lysine residue of another ubiquitin or ubi-tag, forming a ubi-tag dimer linked via an iso-peptide bond. (b) Schematic representation of the general CRISPR/HDR hybridoma genome editing approach for the generation of ubi-tagged Fab fragments where ubiquitin (red) is fused to the C-terminus of the heavy chain of a Fab (green) followed

by a His-tag (purple). (c) The IgH locus of KT3 is targeted for double strand break by gRNA_H to allow the integration of the homology directed repair (HDR) template consisting of a ubi-tag, His-tag, an internal ribosomal entry site (IRES) and blasticidin resistance gene (BSR) (d) Flow cytometry screening of clonal supernatants of the CRISPR/HDR targeted cells following limiting dilution, showing EL4 cells expressing mCD3 incubated with the supernatants followed by anti-his secondary antibody. (e) SDS-PAGE analysis of purified Fab-Ub in the absence or presence of β -mercaptoethanol, stained with Coomassie Blue and analyzed by western blot using an anti-Ub antibody. (f) Coomassie staining and western blot analysis of hybridoma culturing media containing ubi-tagged Fab after 2 and 5 days in presence or absence of Ubiquitin-propargylamide (Ub-PA). (g) Antigen binding competition assay of murine CD3 Fab-Ub against fluorescently-labeled parental mAb of the same clone. Representative of n=3 independent experiments.

Isolation and functional characterization of ubi-tagged antibody fragments

After expansion, the modified hybridoma cells were cultivated for antibody fragment production for 7 to 10 days. After cultivation, we observed that the ubi-tagged Fabs partially or fully lost the C-terminal His-tag, depending on the duration in which the hybridoma cells were cultivated. We hypothesized that the C-terminal His-tag is possibly lost during culture due to deubiquitinating enzymes (DUBs) released by dying cells into the culturing media cleaving the His-tag from the C-terminus of ubiquitin^{39–41}. To test this, we cultivated the modified hybridoma cells in presence or absence of C-terminally propargylated ubiquitin (Ub-PA), known to selectively inhibit cysteine DUBs, and detected the presence of the His-tag on the ubi-tagged Fab secreted in the supernatant at day 2 and 5 of cultivation by anti-his western blot analysis. In absence of Ub-PA in the culture media, on day 2 a thin band was observed by western blot analysis which decreased in intensity by day 5 (Fig 1f). Also when the ubi-tagged Fab containing supernatants were visualized by coomassie, in absence of Ub-PA, two bands were observed corresponding to Fab-Ub-his and Fab-Ub. However, in presence of Ub-PA in the culture media, a single band is observed by Coomassie and on western blot the intensity of the band increased, indicating that indeed the loss of the His-tag during cultivation can be resolved by supplementing the culture medium with 1 μM Ub-PA (Fig. 1f). Following cultivation and isolation of the ubi-tagged Fab-fragment, we performed a competitive antigen binding assay to confirm that the ubi-tagged Fab-fragment retained antigen binding. Here, we used the CD3 expressing cell line EL442 to compete a fixed concentration of fluorescently labeled parental antibody against increasing concentrations of unlabeled ubi-tagged Fab CD3. The ubi-tagged Fab competed with the fluorescent parental antibody in a dose-dependent manner, indicating that antigen binding was retained (Fig. 1g).

Site-specific fluorescent labeling of ubi-tagged Fab fragments

Having validated that the binding of a ubi-tagged antibody fragment to its cognate antigen is retained, we next set out to determine the feasibility of using ubiquitin as a conjugation tag. Three main determinants crucial for the specificity of ubi-tag conjugation are: (1) the ubiquitinating enzymes specific for a single lysine linkage-

type, (2) the acceptor ubi-tag (ub^{acc}) carrying the corresponding lysine residue while having an unavailable C-terminal glycine, and (3) the donor ubi-tag (Ub^{don}) having a free C-terminal glycine while the conjugating enzyme-specific lysine is mutated. This design ensures that the two different ubi-tagged moieties are only conjugated to one another and prevents either of them from being conjugated to a similar ubi-tag moiety (Fig. 2a).

To assess the efficiency of using ubiquitin as a conjugation tag for the introduction of a payload to the ubi-tagged Fab, we used a donor ubi-tagged Fab, hereafter referred to as Fab-Ubdon, and a chemically synthesized acceptor ubiquitin carrying a rhodamine fluorophore on its N-terminus, hereafter referred to as Rho-Ubacc (Fig. 2a and Supplementary Fig. 1). For this conjugation reaction, the lysine-48 (K48)-specific ubiquitin E2-E3 fusion protein gp78RING-Ube2g2 was used36. To validate our design and confirm that no self-tagging occurs, the ubi-tag conjugation was carried out in the presence or absence of the donor and acceptor ubi-tag, respectively. In the presence of both Rho-Ubacc and Fab-Ubdon, a single fluorescent band was observed after 30 minutes, indicating the formation of a single product corresponding to a Fab attached to a fluorescent label through ubiquitin chain formation (Fig. 2b). In the absence of either Rho-Ubacc or Fab-Ubdon, no product formation was observed. In the absence of Rho-Ubacc, the band shifting upwards at around 90 kDa after 30 minutes on Coomassie corresponds to the molecular weight of Fab-Ubdon loaded on the E2-E3 enzyme. The product of the conjugation reaction, fluorescently labeled Fab (hereafter Rho-Ub₃-Fab), was purified using Protein G affinity purification and analyzed using ESI-TOF mass spectrometry (Fig. 2b). The disappearance of the mass peak corresponding to the mass of Fab-Ub^{don} indicated that it was completely consumed in the conjugation reaction and the mass observed corresponded to the calculated mass of the covalently attached Rho-Ub₂-Fab (Fig. 2b). The efficiency of ubi-tag conjugation reactions carried out in the scope of this study were quantified, showing an average efficiency of 94% for all reactions involving ubi-tagged Fab fragments (Supplementary Fig. 2). To assess the effect of ubi-tag conjugation on protein stability, we compared the thermal unfolding profiles of Rho-Ub₂-Fab to that of the unconjugated Fab-Ub^{don}. We monitored the temperature-dependent change in intrinsic protein fluorescence to determine the infliction temperature at which the protein unfolds. Both conjugated and unconjugated ubi-tag Fab showed an infliction temperature of about 75 °C, indicating that ubi-tagging does not alter protein stability (Fig. 2c). Next, we used flow cytometry to compare the staining of CD3 positive mouse splenocytes with Rho-Ub₃-Fab CD3 to the staining with FITC-labeled parental antibody (Fig. 2d). Both Rho-Ub₃-Fab CD3 and FITC labeled parental antibody showed a comparable percentage of CD3-positive cells, illustrating that ubi-tag conjugation does not hinder antigen binding.

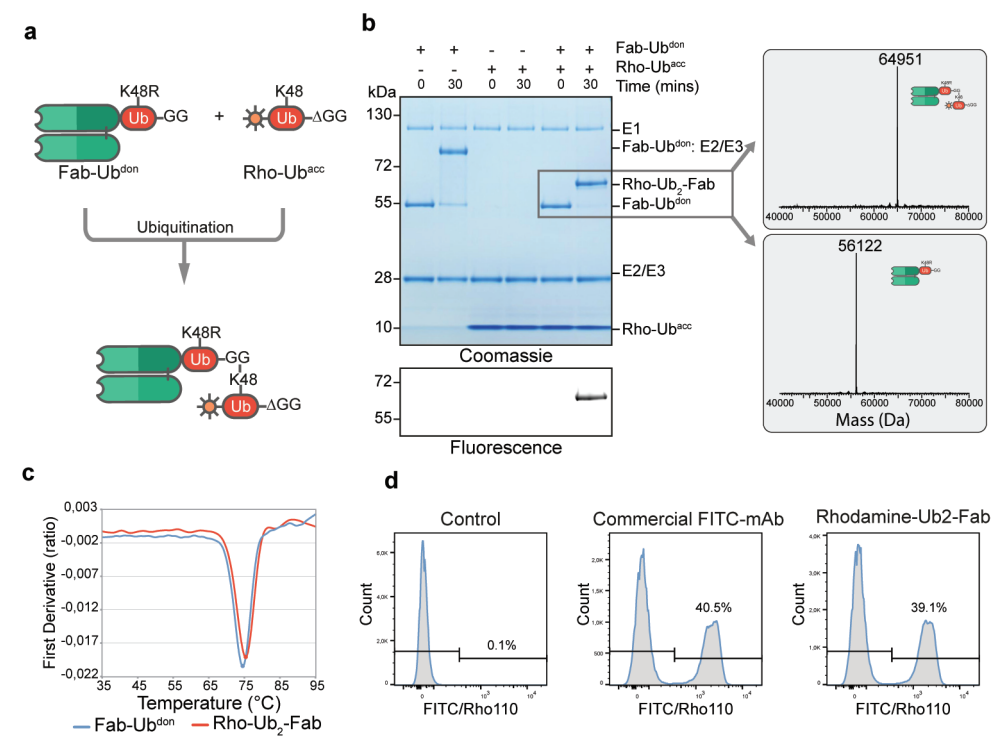


Figure 2 | Ubi-tag conjugation for the site-specific fluorescent labeling of a ubi-tagged Fab fragment (a) Schematic representation of the concept of K48-specific ubi-tag conjugation for the fluorescent labeling of Fab-Ub. (b) Labeling of Fab-Ub^{don} with Rho-Ub^{acc} using K48-specific ubiquitination enzymes shown by non-reducing SDS-PAGE followed by fluorescent imaging and Coomassie Blue staining. The deconvoluted ESI-TOF mass spectrum of the Fab fragments isolated from the reaction mixture confirmed the conjugation of all Fab-Ub^{don} to form Rho-Ub₂-Fab. (c) Thermal unfolding profiles of Fab-Ub (blue) and the conjugated Rho-Ub₂-Fab (red) showing similar thermostability. (d) Histograms of mouse splenocytes showing the percentage CD3 positive cells stained with Rho-Ub₂-Fab CD3 or FITC-mAb CD3 analyzed by flow cytometry.

Bi-and tri-valent antibody formats using ubi-tag conjugation

Having established and validated ubi-tag conjugation for antibody fragments, we next decided to assess the production of multimeric antibody formats using ubi-tag conjugation. We first evaluated the upper limit for the multimerization reaction efficiency, using a ubi-tagged Fab where the fused ubiquitin has both the acceptor lysine available as well as a free C-terminal glycine (hereafter referred to as Fab-Ub^{WT}) to allow the formation of higher-order ubiquitin chains (Fig. 3a). Within 30 minutes of the conjugation reaction, the majority of Fab-Ub^{WT} was converted to multimeric Fab-Ub chains, showing the feasibility of the ubiquitination enzymes to elongate the Fab-Ub chains forming multimers as high as the 11th order and beyond, indicating that a large cargo such as a Fab of 50 kDa does not hamper ubi-tag conjugation (Fig. 3b and Supplementary Fig. 3).

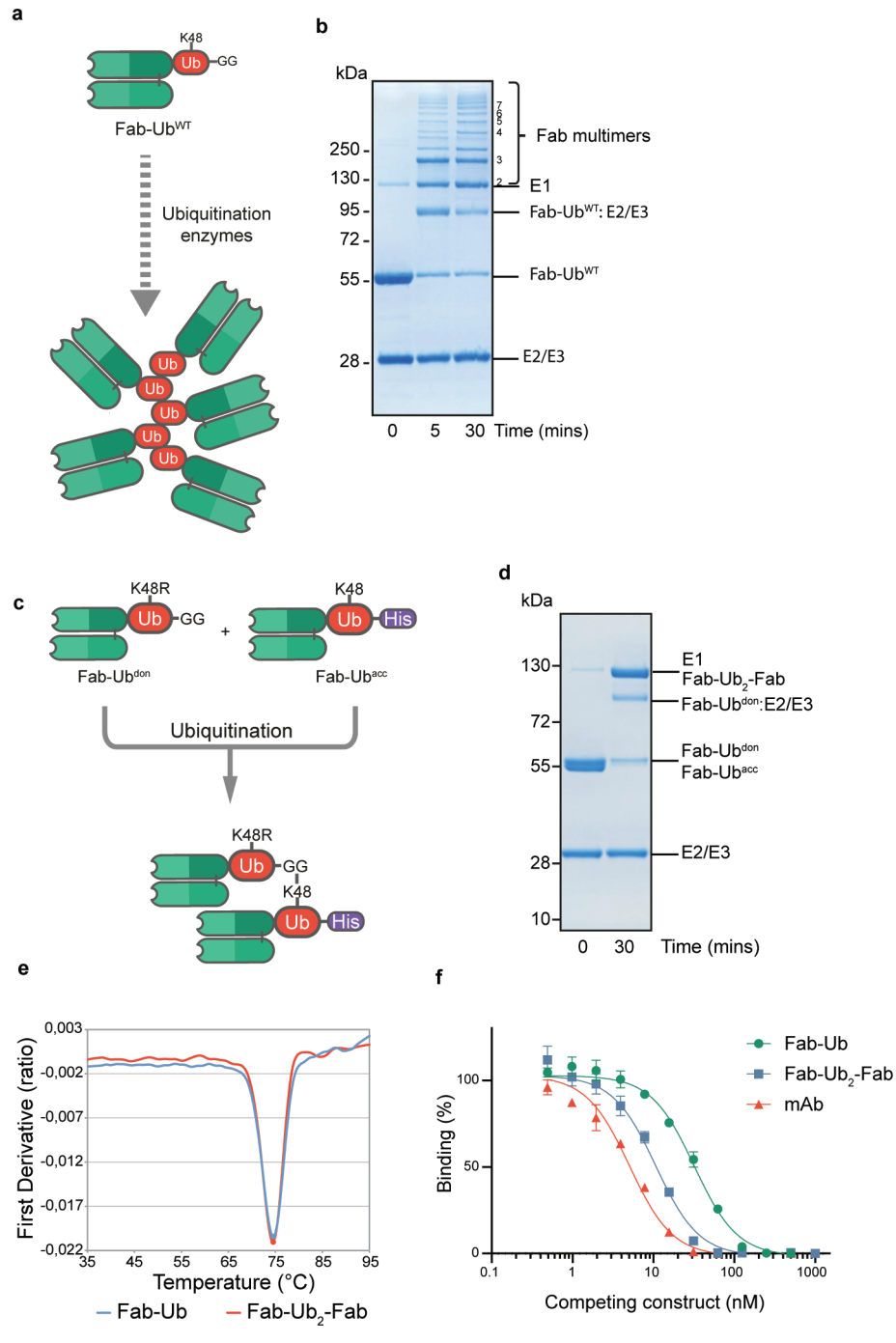


Figure 3| Site-specific Fab multimerization and dimerization through ubi-tag conjugation. (a) Schematic overview of ubi-tag based multimerization reaction of Fab-Ub^{WT}, where both the C-terminal glycine residue as well as lysine 48 are available for conjugation. (b) Non-reducing SDS-

PAGE gel stained with Coomassie Blue visualizing multimerization of Fab-UbWT in 30 minutes. (c) Schematic diagram of site-specific heterodimerization of ubi-tagged Fab-fragments. (d) Non-reducing SDS-PAGE analysis of site-specific conjugation to generate Fab-Ub2-Fab. Here, both ubi-tagged Fab moieties target mCD3. (e) Thermal unfolding of Fab-Ub2-Fab (red) compared to Fab-Ub (blue) showing that dimerization does not compromise the stability of the ubi-tagged Fab fragment. (f) Competition binding assay of each of Fab-Ub (green), Fab-Ub2-Fab (blue), and parental mAb (red) targeting mCD3 against fluorescently labeled parental mAb. Representative experiment of n=3, each condition performed in triplicates. Data are shown as mean ±SD.

Next, we set out to make a bivalent monospecific Fab-Ub₃-Fab against mouse CD3. The monospecific Fab heterodimer was efficiently generated by conjugating a Fab CD3-Ubacc, with a His-tag blocking the C-terminal glycine, to a Fab CD3-Ubdon with a UbK48R mutation (Fig. 3c and 3d). The resulting Fab-Ub₂-Fab was assessed for its thermostability compared to the Fab-Ub monomer. Indeed, dimerization did not influence the thermostability compared to the monomer (Fig. 3e). To validate the functionality and assess the avidity effect of the bivalent antibody format compared to the monovalent Fab-Ub, a competition binding assay was performed using EL4 cells expressing mouse CD3 (Fig. 3f). For this, we competed a fixed concentration of fluorescentlylabeled parental antibody against increasing concentrations of Fab-Ub, Fab-Ub₂-Fab, and unlabeled parental antibody. Fab-Ub₃-Fab showed a lower IC₅₀ compared to the monovalent Fab-Ub which we attribute to the increased avidity of the bi-valent format. Next, we set out to investigate the feasibility of site-specific ubiquitin chain elongation of the hetero-dimeric Fab-Ub₂-Fab to form a hetero-trimer. We reasoned that exposing the C-terminal glycine of the Ubacc of the Fab dimer would transform it into a Fab-Ub₂don-Fab, allowing it to be available for conjugation to a third Ubacc moiety (Fig. 4a). For this purpose, we used the deubiquitinating enzyme (DUB) UCHL3, known to exclusively liberate the C-terminus of Ub and not the isopeptide linkage in the Ub,, to cleave the His-tag from the C-terminus of the Ub, 40,41,43. The cleavage reaction was monitored by mass spectrometry, detecting a decrease in mass of the heavy chain dimer of 1371 Da, corresponding to the His, tag being cleaved off (Fig. 4b). Following isolation from the reaction mixture, the Fab-Ub₂don-Fab, now carrying an available C-terminus, was conjugated to Rho-Ubacc . Also this reaction showed to be highly efficient, where after 30 minutes almost all heavy chain dimer was conjugated to Rho-Ubacc as shown by Coomassie staining and fluorescent scan of the protein gel ran in reducing conditions (Fig. 4c). Similarly, the heterotrimer formation by conjugating Fab-Ub₂don-Fab to a third Fab fused to a Ubacc proved to be efficient, showing that the majority of the dimer converted into a trimer after 30 minutes (Fig. 4d).

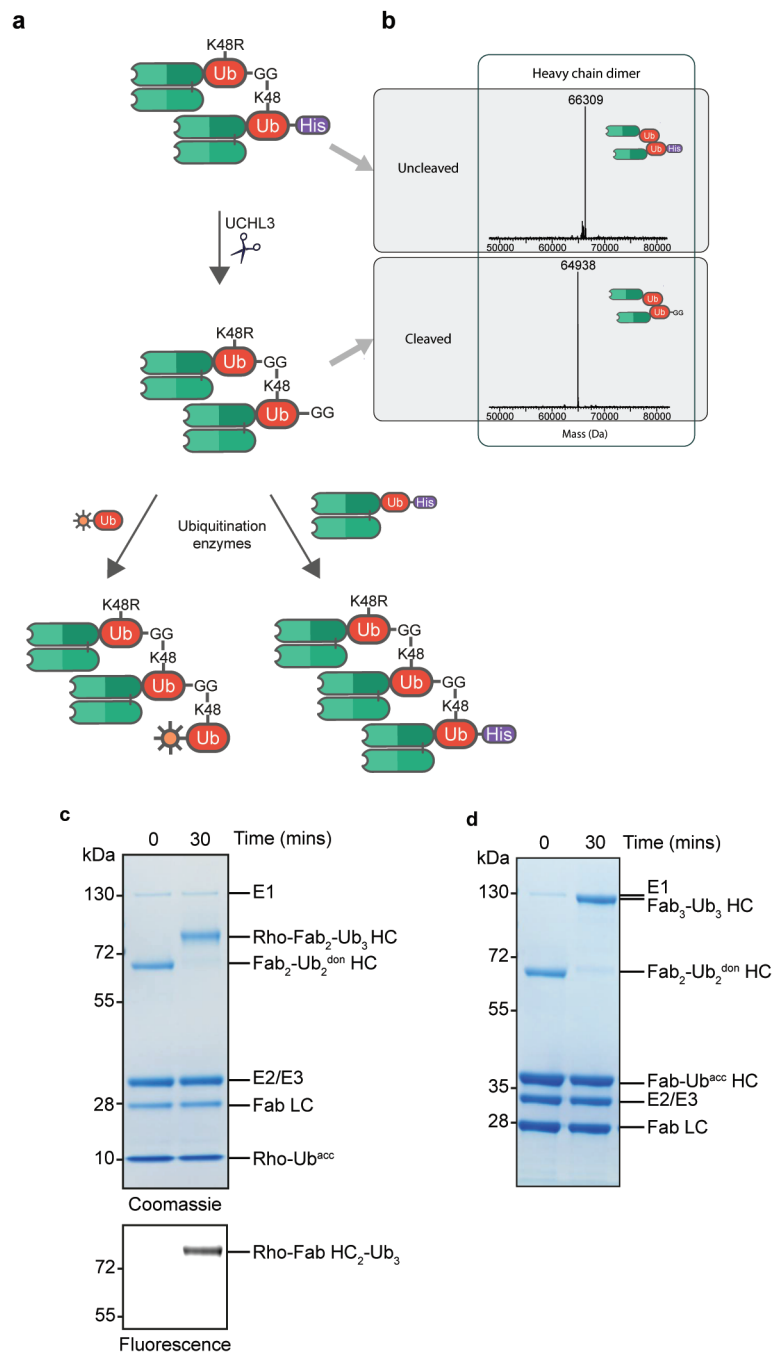


Figure 4| Generation of heterotrimeric ubi-tagged antibody complexes (a) Schematic illustration of ubiquitin chain elongation to form hetero-trimeric antibody complexes (b) Deconvoluted ESI-TOF mass spectra of the heavy chain dimer of Fab-Ub₂-Fab and Fab-Ub₂^{don}-Fab, showing the liberation of the His₁₀-tag from Fab-Ub₂-Fab by UCHL3 (calculated mass different = 1371 Da, observed mass difference =

1371 Da). (c) Conjugation of Fab-Ub₂^{don}-Fab to Rho-Ub^{acc} analyzed by SDS-PAGE in reducing conditions followed by fluorescent imaging and Coomassie Blue staining. (d) Reducing SDS-PAGE analysis showing the conjugation of the heterodimer Fab-Ub₃^{don}-Fab to Fab-Ub^{acc} to form a Fab heterotrimer.

Ubi-tag conjugation is site-specifically reversible by DUBs

Lastly, we set out to investigate whether the internal isopeptide bond in the generated ubi-tagged conjugates were recognized and processed by deubiquitinating enzymes. We reasoned that cleaving ubi-tagged conjugates could potentially further expand the applications of this technology when used in a context where the controlled disassembly of the conjugate is desirable (Fig. 5a). However, the presence of DUBs in a biological setting could also be detrimental to the stability and functionality of the ubi-tagged conjugates. To investigate whether DUBs are capable of cleaving ubi-tagged conjugates, we selected OTUB1, a DUB known to have a preference for cleaving K48-linked ubiquitin chains⁴⁴, and assessed its effect on the K48-linked Rho-Ub₃-Fab when incubated together over time by Coomassie staining and fluorescent scan of the protein gel. As shown in figure 5b, the fluorescence intensity of the upper band corresponding to Rho-Ub₂-Fab decreases over time while a lower band running around 10kDa corresponding to Rho-Ub appears and increases in intensity. Similarly, on Coomassie over time the upper band corresponding to Rho-Ub,-Fab decreases in intensity while two bands at around 55kDa and 10 kDa appear and increase in intensity, corresponding to Fab-Ub and Rho-Ub respectively. This indicated that the K48-linked Rho-Ub₂-Fab was processed and cleaved by OTUB1. Next, we investigated the stability of Rho-Ub₃-Fab in human serum in vitro as a preliminary indication for the usability of ubi-tag conjugation for diagnostic or therapeutic applications. Here, we monitored the stability of Rho-Ub₃-Fab when incubated in human serum in vitro at 37°C over 24 hours (Fig. 5c). Notably, the band corresponding to Rho-Ub₃-Fab remained equal in intensity over time while no new bands appeared indicating that Rho-Ub₂-Fab remained stable in human serum in vitro for more than 24 hours. To validate that a ubi-tagged Fab conjugate carrying a larger cargo such as a ubi-tagged Fab-dimers could still be processed by DUBs, we incubated the K48-linked Fab-Ub,-Fab with OTUB1 and monitored its stability over time (Fig. 5d and 5e). After 90 minutes, the majority of Fab-Ub₃-Fab was cleaved and a band corresponding to the Fab-Ub monomers could be observed indicating that larger ubitagged conjugates such as Fab-Ub₃-Fab are still recognized and cleaved by OTUB1.

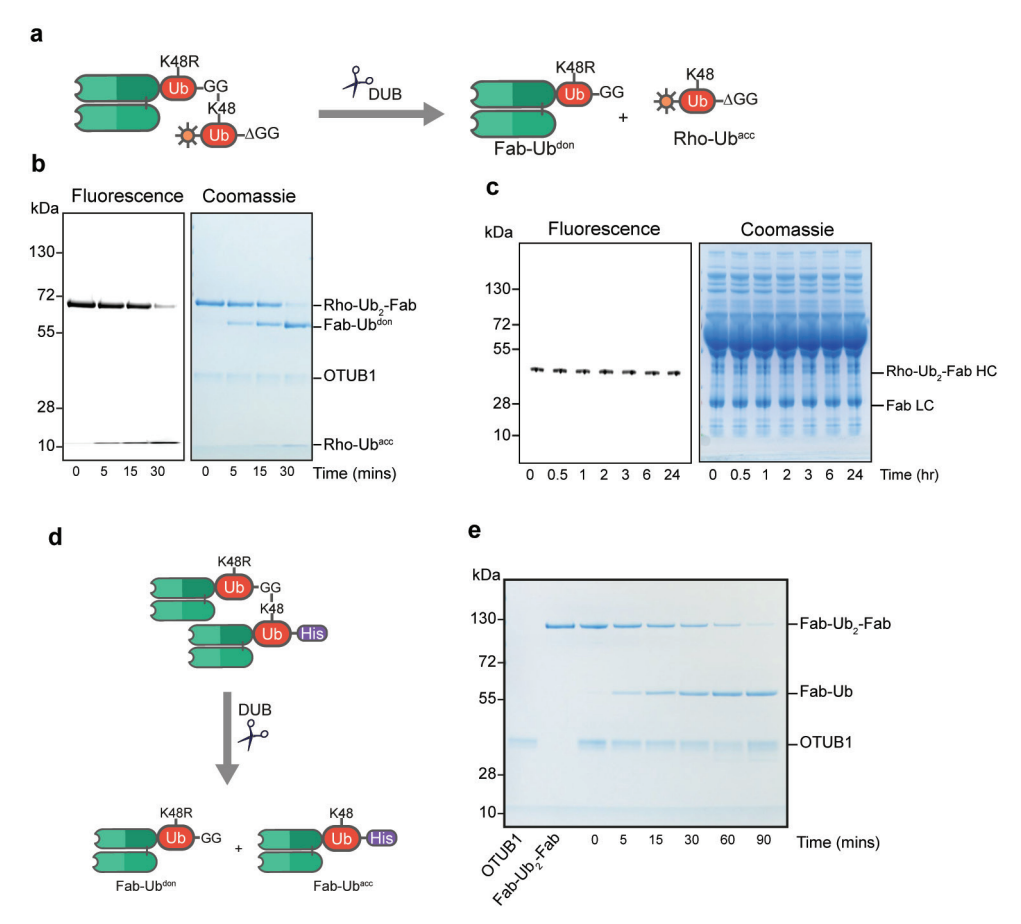


Figure 5| Site-specific disassembly of ubi-tagged antibody conjugated by DUBs. (a) Schematic representation of the disassembly of K48 linked Rho-Ub₂-Fab by deubiquitinating enzymes to form the monomers Fab-Ub^{don} and Rho-Ub^{acc}. (b) Cleavage of Rho-Ub₂-Fab by the K48-specific DUB OTUB1 shown by non-reducing SDS-PAGE followed by fluorescent imaging and Coomassie Blue staining. (c) In vitro stability of Rho-Ub₂-Fab in human serum analysed by SDS-PAGE in reducing conditions, visualized by fluorescent imaging and Coomassie Blue staining. (d) Schematic illustration of Fab-Ub₂-Fab cleaved by DUBs to form the Fab-Ub^{don} and Fab-Ub^{acc} monomers. (e) K48-linked Fab-Ub₂-Fab cleavage by OTUB1 analyzed by non-reducing SDS-PAGE followed by Coomassie blue staining.

mAb conjugation and Tetravalent antibody formats

To show that ubi-tagging is not restricted to antibody fragments but can also be applied to full mAbs, we produced recombinant mAbs with a ubi-tag fused to the C-terminus of each heavy chain. We produced two ubi-tagged mAbs, TA99 anti-TRP1 carrying an acceptor ubi-tag and 2C11 anti-mCD3 carrying a donor ubi-tag. We generated the ubi-tagged anti-TRP1 mAb using the hybridoma genome editing technology³⁸, where we targeted the hinge region of the TA99 anti-TRP1 hybridoma to introduce an Fc-silent domain to which acceptor ubiquitin (Ub Δ GG) was fused. The Fc-silent domain

was introduced to avoid Fc-mediated immune activation in the following applications. Stable ubi-tagged antibody-producing hybridoma clones were obtained, and Ubi-tagged mAbs were validated for the presence of the ubi-tag using western blot analysis (Supplementary Fig. 4). The ubi-tagged 2C11 anti-mCD3 mAbs were generated by overexpression of the mAbs in HEK-293 cells. Here, the Fc-silent domain was also introduced to which the donor ubi-tag was fused. Both ubi-tagged mAbs were purified

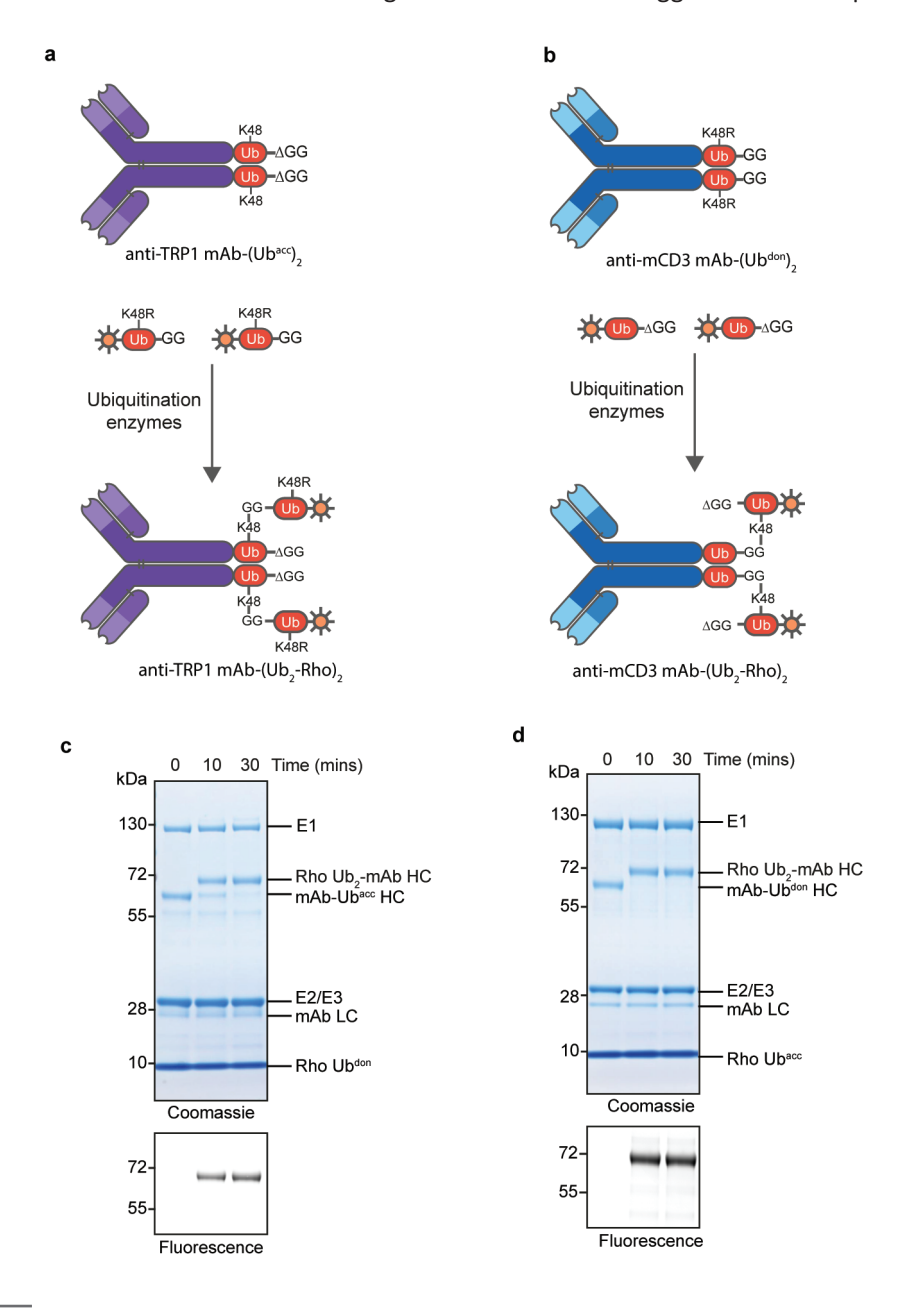


Figure 6| Ubi-tag conjugation for the fluorescent labeling of ubi-tagged mAbs (a) Schematic representation of the K48-specific ubi-tag conjugation for the fluorescent labeling of anti-TRP1 mAb-Ubacc to Rho-Ubdon. (b) Schematic representation of the ubi-tag conjugation of anti-mCD3 mAb-Ubdon to Rho-Ubdon to anti-TRP1 mAb-(Ubacc), analyzed by SDS-PAGE under reducing conditions and visualized by fluorescent imaging and Coomassie Blue staining. (d) Conjugation of Rho-Ubdoc to anti-mCD3 mAb-(Ubdon), analyzed by SDS-PAGE under reducing conditions and visualized by fluorescent imaging and Coomassie Blue staining.

using Protein A affinity purification and the purified ubi-tagged mAbs were assessed by mass spectrometry (Supplementary Fig. 5).

To assess the conjugation efficiency of ubi-tagged mAbs and determine if full conjugation is achievable, we decided to first test the ubi-tag conjugation of both donor and acceptor ubi-tagged mAbs to a ubitag carrying a small cargo, a rhodamine moiety, to either an acceptor or donor respectively (Fig. 6a-b). We tested the conjugation of the mAb fused to an acceptor ubiquitin, hereafter mAb-(Ubacc), to Rho-Ubdon. After 30 minutes, the heavy chains of mAb-(Ubacc), were fluorescently labeled as shown by Coomassie staining and fluorescent scan in figure 6c. The protein gel was run in reducing conditions, and it can be appreciated that the complete upward shift of the band corresponding to the ubi-tagged heavy chain indicates that both ubi-tags on each of the heavy chains were conjugated to Rho-Ub. To confirm that ubi-tagged mAbs can be efficiently conjugated in both acceptor and donor ubi-tag formats, we conjugated a mAb-(Ubdon), to Rho-Ubacc. Indeed, both ubi-tagged mAb formats showed similarly high conjugation efficiency (Fig. 6d).

Next, we attempted to form a tetravalent bispecific-antibody conjugate applying ubi-tagging. We aimed for a bispecific T cell engager (BiTE) in two ubi-tagged formats, one by conjugating anti-TRP1 Fc-silent mAb-(Ubacc), to anti-mCD3 (clone 145-2C11) Fab-Ubdon and the other by conjugating anti-mCD3 Fc-silent mAb-(Ubdon), to anti-TRP1 Fab-Ubdon (Fig 7a-b). The conjugation reactions reached near completion in 60 minutes (Fig. 7c-d) in which the majority of the unconjugated mAb-(Ub), were converted to the tetravalent bispecific-antibody conjugate mAb-(Ub3-Fab)3. After purification the functionality of these two ubi-tagged BiTEs were evaluated in an in vitro T cell activation and cytotoxicity assay. Here, WT or TRP1 transfected KPC3 cells (KPC3-TRP1) were co-cultured with CD8 T cells from WT C57BL6/J mice and incubated with increasing concentrations of either of the two bispecific antibody complexes or the combination of their corresponding unconjugated mAb-(Ubacc), and Fab-Ubdon(Fig.7e-f). Flow cytometry analysis revealed that both ubi-tagged BiTEs induced a dose-dependent T cell activation as measured by the increased expression of Ki67, granzyme B, CD69 and 4-1BB (CD137) by the T cells, only when co-cultured with KPC3-TRP1 cells and not with KPC3 WT cells (Fig. 7e-f and Supplementary Fig. 6). Additionally, the ubi-tagged BiTEs showed a dosedependent cell killing in an LDH release assay with TRP1 expressing KPC3 cells, while the WT cells and KPC3-TRP1 incubated with the unconjugated mAb-(Ubacc), and Fab-Ubdon showed no induction of killing (Fig. 7e-f and Supplementary Fig. 7). Altogether these results demonstrate the flexibility and efficiency of the ubi-tagging approach, and the functionality of ubi-tagged tetravalent bispecific-antibody complexes.

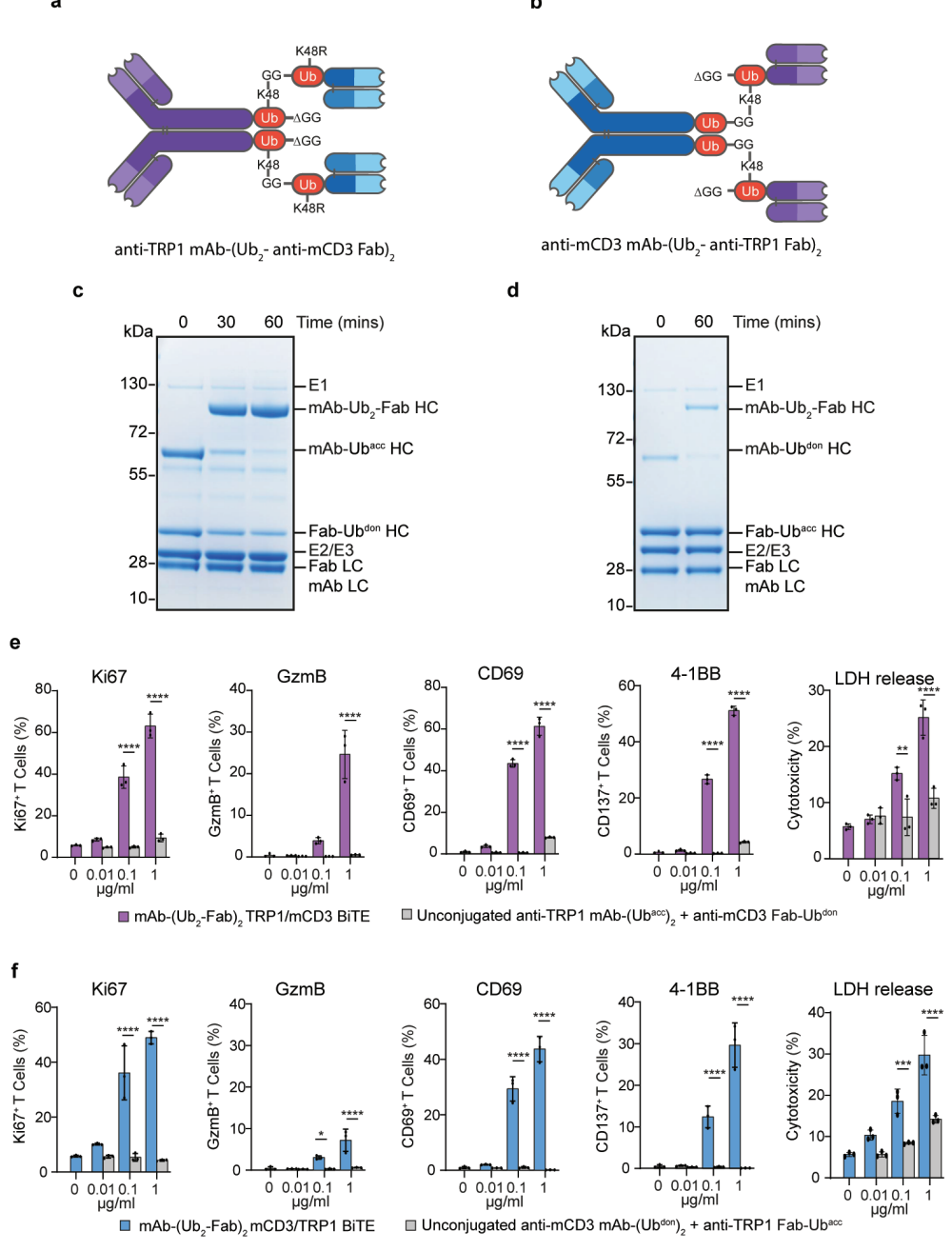


Figure 7 | Conjugation of ubi-tagged mAbs for the generation of a bispecific tetravalent antibody

complexes. (a) Schematic representation of anti-TRP1 mAb-(Ub₂-anti-mCD3 Fab)₂ generated by ubitag conjugation of anti-TRP1 mAb-(Ubacc), to two moieties of anti-mCD3 Fab-Ubdon. (b) Schematic representation of the bispecific tetravalent antibody complex anti-mCD3 mAb-(Ub₂-anti-TRP1 Fab) by ubi-tag conjugation of anti-mCD3 mAb-(Ubdon), to two moieties of anti-TRP1 Fab-Ubacc. (c) SDS-PAGE analysis of the generation of the bispecific tetravalent antibody complex anti-TRP1 mAb-(Ub.anti-mCD3 Fab), by ubi-tag conjugation of anti-TRP1 mAb-(Ubacc), to two moieties of anti-mCD3 Fab-Ubdon. (d) SDS-PAGE analysis of the generation of the bispecific tetravalent antibody complex antimCD3 mAb-(Ub,-anti-TRP1 Fab), by ubi-tag conjugation of anti-mCD3 mAb-(Ubdon), to two moieties of anti-TRP1 Fab-Ubacc, (d-h) In vitro T cell activation and cytotoxicity by the ubi-tagged bispecific TRP1xmCD3 complexes. Primary mouse (C57BL/6) CD8+T cells were added in a 10:1 ratio to KPC3-Trp1 followed by addition of $0 - 1 \mu g/mL$ of either mAb-(Ub,-Fab), or unconjugated mAb-(Ub), and two Fab-Ubdon, and incubated for two days. T cell activation was assessed using flow cytometry for Ki67, Granzyme B, CD69, and 4-1BB. Data (n=3) are shown as percentage positive T cells ±SD. T tests, ****P<0.0001, **P<0.01. Full statistical analysis is provided in supplementary table S5. Cytotoxicity was assessed using a LDH cytotoxicity assay. Data (n=3) are shown as percentage cytotoxicity ±SD. T tests, ****P<0.0001, **P<0.01. Full statistical analysis is provided in supplementary table S5.

Discussion

Over the past decade, tremendous advances have been made in the field of antibody conjugation to facilitate the generation of antibody conjugates and multivalent antibody formats for a broad spectrum of applications in research, diagnostics and therapy. Traditional conjugation methods rely on chemical modification of primary amines or thiol groups along the antibody sequence resulting in heterogenous mixtures with multiple uncontrolled modification sites.^{1–3} This often results in batch-to-batch variability, reduced antigen binding and impaired stability.

Significant progress has been made in the development of site-specific conjugation methods, contributing to innovation in the generation of antibody conjugates of diverse formats. However, slow reaction kinetics, low yield and time-consuming multistep conjugation procedures remain problematic.^{5,17,22} Hence, substantial efforts are currently still being focused on developing new or improved antibody conjugation strategies.

Here we report the use of ubiquitin conjugation (ubi-tagging), as a highly-specific and broadly applicable antibody conjugation platform. We demonstrate that this approach is an efficient technology for the site-specific, and flexible ubi-tag conjugation. In this study we addressed four main aspects of this technique: (1) Ubi-tag conjugation reactions result in a highly defined homogenous product that is covalently attached at a specific position. For the conjugation reactions, we used an E2-E3 fusion enzyme specific for ubiquitin conjugation on lysine 48 and a single product was formed in each reaction (Fig. 2b). This indicates that the conjugation only took place on lysine 48 and that a defined antibody conjugate was produced that, in contrast to commonly used conjugation techniques, is consistent from batch-to-batch. (2) Ubi-tag conjugation reactions are fast and highly efficient process. The efficiency of ubi-tag conjugation reactions in this study at timepoint 30 minutes were quantified and plotted (Supplementary Fig. 2).

Conjugation reactions involving ubi-tagged Fab fragments or ubi-tagged mAbs showed an average reaction efficiency of 93% and 96%, respectively. This indicates that the ubitag conjugation reaction efficiency was not hampered, neither as donor nor acceptor ubi-tag, by fusion to a protein with molecular weight as high as a mAb of 150 kDa. (3) The specificity and efficiency of ubi-tag conjugation facilitates the generation of multimeric antibody complexes with an unprecedented ease. The level of control in this conjugation reaction, with a defined donor ubi-tag and acceptor ubi-tag each fused to a different moiety, allows the generation of defined hetero-multimeric antibody complexes (Fig 3, 4 and 7). (4) The established full chemical synthesis of ubiquitin^{45–47} further expands its potential applications as an antibody conjugation tag. This facilitates the attachment of chemical modifications such as small molecules, fluorophores, tags or chemical warheads at one or more position in a defined manner (Fig. 2, 6 and Supplementary Fig. 1).

Although, in this study the K48 specific E2-E3 pair gp78RING-Ube2g2 was used³⁶, ubi-tag conjugation is not limited to this pair of ubiquitin E2 and E3 enzymes or linkage type. Other E2 and E3 enzymes also proved to be exploitable for ubi-tag conjugation of proteins and antibodies, including the E2-E3 pair UbcH7 and NIeL⁴⁸ for the generation of K6-linked ubi-tagged antibody conjugates (Supplementary Fig. 8). The variety in ubiquitin linkage types and linkage specific ubiquitination enzymes provide additional flexibility to this conjugation platform. Additionally, ubiquitin chains of different linkage types are known to have different conformations²⁶. This could be exploited in future research for applications where it is of value to gain control over the spatial orientation of the antibodies conjugated to each other⁴⁹. Furthermore, another promising aspect of ubi-tag conjugation is its specific reversibility using deubiquitinating enzymes⁵⁰(Fig. 5). Conditional cleavage using DUBs, could provide dynamic control over the activity of ubi-tagged antibody complexes.

In summary, ubi-tag conjugation provides a fast, efficient, and modular technique to generate well-characterized antibody conjugates of limitless formats and combinations. We expect the widespread adoption of this conjugation technique and its contribution to improving and developing antibody conjugates for preclinical research, diagnostic, and therapeutic applications.

Methods

General cell culture conditions

The hybridoma cell line KT3, kindly provided by dr. Ramon Arens (LUMC, The Netherlands), was modified for the stable expression of ubi-tagged antibodies or antibody fragments. Other cell lines used in this study were EL4 (kindly provided by dr. Jacques Neefjes (LUMC, The Netherlands) KPC3 and KPC3-TRP1. KT3 and EL4 cells were cultured in Dulbecco's modified Eagle's medium (DMEM) (Gibco) supplemented with 7.5% FCS. The KPC3 cell line was obtained from a primary pancreatic KPC tumor with mutant p53 and K-ras⁵¹

from a female C57BL/6 mouse. KPC3-Trp1 was generated as described 52 and purified using cell sorting with the TA99 antibody. Cells were cultured in IMDM supplemented with 7.5% FCS. All the cell lines used in the study were maintained at 37 °C and 5% CO $_2$, routinely examined by morphology analysis and tested for mycoplasma.

Cloning of CRISPR-Cas9 and donor constructs

The genomic sequence of the rlgG2a heavy chain locus, mlgG2a heavy chain locus, were identified via the Ensembl rate genome build Rnor 6.0 and used for the design of the different HDR donor templates. gRNA for the rlgG2a constructs were previously described; for Hinge HDR constructs, gRNA-H, GACTTACCTGTACATCCACA, Addgene 124808; for isotype switch, gRNA-ISO (TGTAGACAGCCACAGACTTG, Addgene 124811). For the hinge region of mlgG2a gRNA-85 (TGGAGGACAGGGCTTGATTG), gRNA-76 (GGGCTTGATTGTGGGCCCTC) and gRNA-102 (TTACCTGGGCATTTGCATGG) were designed using the CRISPR tool from the Zhang laboratory (http://crispr.mit.edu) and ordered as single-stranded oligos from Integrated DNA Technologies (IDT) with the appropriate overhangs for cloning purposes. The oligos were phosphorylated with T4 PNK enzyme by incubation at 37 °C for 30 minutes and annealed by incubation at 95 °C for 5 minutes followed by gradually cooling to 25 °C using a thermocycler. The annealed oligos were cloned into the plasmid pSpCas9(BB)-2A-Puro (PX459), which was obtained as gifts from F. Zhang (Addgene plasmids 62988)⁵³. Synthetic gene fragments containing homologous arms and desired insert were obtained via Twistbioscience and cloned into the PCR4 TOPO TA vector (Thermo Fisher Scientific). All CRISPR-Cas9 and HDR constructs were purified with the NucleoBond Xtra Midi Kit (740410.100, Machery-Nagel) according to the manufacturer's protocol.

Hybridoma nucleofection with HDR and CRISPR-Cas9

Nucleofection of the HDR template and CRISPR-Cas9 vectors was performed with Cell Line Nucleofector Kit R (Lonza, VCA-11001) nucleofector 2b device. Before nucleofection hybridoma cells were assessed for viability and centrifuged (90g, 5 minutes), resuspended in PBS supplemented with 1% FBS and centrifuged again (90g, 5 minutes). 1x10⁶cells were resuspended in 100 μL Nucleofector medium with 1 μg of HDR template and 1 μg of CRISPR-Cas9 vectors or 2 μg of GFP vector (control) and transferred to cuvettes for nucleofection with the 2b Nucleofection System from Lonza (Program X001). Transfected cells were transferred to a 6-well plate in 4 mL of prewarmed complete medium. The following day the cells were transferred to a 10 cm petridish in 10 mL of complete medium, supplemented with 10-20 μg/mL of blasticidin (Invivogen, anti-bl-05). Antibiotic pressure was sustained until GFP-transfected hybridomas were dead and HDR transfections were confluent (typically between day 10-14). Cells were subsequently clonally expanded by seeding the hybridomas in 0.3

cells/well in round-bottom 96-well plates in 100 μL of complete medium. After one-two weeks, supernatant from wells with a high cell density were obtained for further characterization and selected cloned were expanded.

Solid-phase peptide synthesis

Solid-phase peptide synthesis (SPPS) of Rho-Ub was performed on a Syro II Multisyntech Automated Peptide synthesizer (SYRO robot; Part Nr: S002PS002; MultiSyntech GmbH, Germany) on a 25 μ mol scale using standard 9-fluorenylmethoxycarbonyl (Fmoc) based solid phase peptide chemistry based on the procedure described by El Oualid *et al.*⁴⁵ using a fourfold excess of amino acids relative to pre-loaded Fmoc amino acid trityl resin (between 0.17 and 0.20 mmol/g, Rapp Polymere, Germany). To prepare Rho-Ub, 5-carboxyrhodamine110 (Rho) was coupled to the N-terminus of Ub following SPPS as described by Geurink *et al.*⁵⁴. All synthetic products were purified by RP-HPLC on a Waters preparative RP-HPLC system equipped with a Waters C18-Xbridge 5 μ m OBD (10 x 150 mm) column. The purified products were lyophilized and assayed for purity by high resolution mass spectrometry on a Waters Acquity H-class UPLC with XEVO-G2 XS Q-TOF mass spectrometer and by SDS-PAGE analysis.

Thermal unfolding assay

For each of the Ubi-tagged Fab and conjugates, 10 μ L samples were prepared with a concentration ranging from 0.5 to 1 mg/mL and loaded into the capillaries (NanoTemper Technologies). Changes in tryptophan fluorescence intensity upon protein unfolding was measured using the NanoTemper Tycho NT.6 (NanoTemper Technologies) using an increasing temperature gradient from 35 °C to 95 °C at a rate of 20 °C/min. The Inflection temperatures (T_i) of the proteins was determined from the first derivative of the fluorescence ratios (F_{350}/F_{330}).

Mass spectrometry

Mass spectrometry analysis was carried out on Waters ACQUITY UPLC-MS system equipped with a Waters ACQUITY Quaternary Solvent Manager (QSM), Waters ACQUITY FTN AutoSampler, Waters ACQUITY UPLC Protein BEH C4 Column (300 Å, 1.7 μ m, 2.1 x 50 mm) and XEVO-G2 XS QTOF Mass Spectrometer (m/z = 200-2500) in ES+ mode. Sample were run using 2 mobile phases: A = 1% MeCN, 0.1% formic acid in water and B = 1% water and 0.1% formic acid in MeCN with a runtime of 14 minutes. In the first 4 minutes, salts and buffer components were flushed from LC column using 98% A and 2% B. In the next 7.5 minutes, a gradient of 2-100% B was used, followed by 0.5 minutes of 100% B and subsequent reduction to 2% B and 98% A in 2 minutes. Data processing was performed using Waters MassLynx Mass Spectrometry Software 4.1, where the mass was obtained by deconvolution with the MaxEnt1 function.

Protein expression and purification

The E1 ubiquitin-activating enzyme UBE1 carrying an N-terminal His-tag was expressed from a pET3a vector in E. coli BL21(DE3) in autoinduction media for 2-3 hours at 37 °C, after which the bacteria were allowed to grow overnight at 18 °C. Next, bacteria were harvested and lysed by sonication, followed by His-affinity purification using Talon metal affinity resin (Clontech Inc., Palo Alto, CA, USA). Subsequently, the protein was further purified by anion exchange using a Resource Q column (GE Healthcare), followed by size exclusion using a Superdex 200 column (GE Healthcare).

The E2/E3 enzyme chimera plasmid was obtained as a gift from dr. Vincent Chau (Penn State, USA). The expression plasmid consists of the RING domain of the E3 ubiquitin ligating enzyme gp78 fused to the N-terminus of the E2 ubiquitin-conjugating enzyme Ube2g2 in a PET28a-TEV vector.

The E2/E3 enzyme chimera was expressed and purified as described 36 . In brief, the fusion protein was expressed in E. coli BL21(DE3) cells grown in LB at 37°C until OD $_{600}$ = 0.4-0.6 and induced with 0.4 mM IPTG for 4 hours at 30 °C. The harvested cells were lysed with Bugbuster protein extraction reagent (Millipore) according to manufacturer's protocol. The fusion protein was purified on Ni-NTA resin followed by size exclusion using a Superdex 200 column (GE Healthcare). Next, TEV protease cleavage was carried out overnight, and the cleaved fusion protein was further purified using a Resource Q column (GE Healthcare).

Ubi-tagged Fabs were produced in hybridoma cell lines engineered to produce Fabs fused at the C-terminus of the heavy chain to ubiquitin, followed by a His-tag at the C-terminus of ubiquitin. The modified hybridoma cells were cultivated for antibody production in CD Hybridoma medium supplemented with 2 mM ultraglutamine and 50 μΜ β-mercaptoethanol for 7 to 10 days. To prevent the cleavage of the His-tag during cultivation, which is essential for blocking the C-terminal glycine residue of acceptor ubi-tags, antibodies fused to an acceptor ubi-tag were secreted in culture media supplemented with Ub-PA. However, donor ubi-tags require a free C-terminus; thus, antibodies fused a donor ubi-tag intended for conjugation were cultured without a DUB inhibitor. After 7 to 10 days, the culture media containing the ubi-tagged Fabs was centrifugated to remove cells. The supernatant was filtered through a 0.22 μm filter (GE Healthcare) and loaded on a pre-equilibrated HiTrap Protein G HP column (GE Life Science), and the ubi-tagged antibodies were purified according to the manufacturer's protocol. Elution fractions containing the ubi-tagged antibodies were pooled and dialyzed against PBS. Acceptor ubi-tagged antibodies, carrying a His-tag at the C-terminus of ubiquitin, were purified by Ni-NTA affinity purification prior to Protein G affinity purification (Supplementary Fig. 9).

Ubi-tag conjugation reaction

Ubi-tag conjugation reactions were carried out in the presence of 0.25 μM E1 enzyme, 20 μM E2/E3 hybrid enzyme, 10 mM MgCl, and 5 mM ATP in PBS. For analysis of the reaction efficiency by SDS-PAGE, an initial reaction sample was taken from the reaction mixture prior to the addition of ATP. After the addition of ATP, the reaction was incubated at 37 °C for 30 minutes while shaking. Conjugation reaction samples were analyzed by quenching 2-5 µL of the reaction mixture in sample buffer and run on 4-12% Bis-Tris gels (Invitrogen) by SDS-PAGE with MOPS as running buffer. All conjugation reactions were run in non-reducing conditions except for conjugation reactions involving constructs of high molecular weight such as Fab trimers, where the sample buffer was supplemented with β-mercaptoethanol. Gels were stained using InstantBlue Coomassie Protein Stain (abcam) and imaged using Amersham600. Fluorescently labeled proteins were visualized by in-gel fluorescence using Typhoon FLA 9500 imaging system (GE Life Sciences) prior to staining with Coomassie. Small-scale reactions were carried out on a scale corresponding to 2.5 µg ubi-tagged antibody fragments, while large-scale reactions were carried out on a 200 μg to 1 mg scale. Ubi-tagged Fab conjugates were purified from the reaction mixture by protein G affinity purification using a HiTrap Protein G HP column (GE Life Science) according to the manufacturer's protocol. The elution fractions containing purified conjugates were pooled, dialyzed against PBS, and concentrated using a 10 kDa Amicon Ultra centrifugal filter unit (Millipore). The purity of the ubitagged conjugates was assessed by SDS-PAGE and high-resolution mass spectrometry on a Waters Acquity H-class UPLC with XEVO-G2 XS Q-TOF mass spectrometer.

For conjugation of α -CD3 Fab-Ub^{don} to Rho-Ub^{acc}, 10 μ M of Fab-Ub^{don} and 50 μ M Rho-Ub^{acc} were used in the reaction. Multimerization of ubi-tagged Fab fragments was carried out using 30 μ M of Fab-Ub^{WT}. For site-specific dimerization of α -CD3 ubi-tagged Fab-fragments, 15 μ M of the Fab-Ub^{don} and 10 μ M Fab-Ub^{acc} were used, and the conjugates were further purified using Ni-NTA prior to dialysis. Rhodamine labeling of ubi-tagged mAbs was carried out using 5 μ M mAbs and 50 μ M Rho-Ub, while bispecific antibody conjugates were generated using 3.5 μ M mAbs and 10 μ M Fab.

Conjugation of a third moiety to ubi-tagged Fab dimer

To prepare Fab-Ub $_2$ -Fab for conjugation, the C-terminal glycine was exposed using the DUB UCHL3. For this, 2.5 μ M Fab dimer was incubated with 50 nM UCHL3 in PBS at 37 °C for 30 minutes. The cleavage efficiency was assessed by high-resolution mass spectrometry on a Waters Acquity H-class UPLC with XEVO-G2 XS Q-TOF mass spectrometer. Following cleavage, UCHL3 was precipitated by 10-fold dilution with 50 mM sodium acetate pH 4.5 and 100 mM sodium chloride, followed by centrifugation. The supernatant containing Fab-Ub $_2$ don-Fab was concentrated, and buffer exchanged to PBS using a 50 kDa Amicon Ultra centrifugal filter unit (Millipore).

For the conjugation of Fab-Ub $_2^{don}$ -Fab to Rho-Ub $_2^{acc}$, 4 μ M Fab-Ub $_2^{don}$ -Fab and 100 μ M Rho-Ub $_2^{acc}$ were reacted in the presence of 0.25 μ M E1 enzyme, 20 μ M E2/E3 hybrid enzyme, 10 mM MgCl $_2$ and 5 mM ATP in PBS for 30 minutes at 37 °C. For the generation of a ubi-tagged Fab trimer, 4 μ M Fab dimer and 30 μ M Fab-Ub $_2^{acc}$ were used for conjugation in the presence of 0.25 μ M E1 enzyme, 20 μ M E2/E3 hybrid enzyme, 10 mM MgCl $_2$ and 5 mM ATP in PBS for 30 minutes at 37 °C. Conjugation reaction samples were analyzed by quenching 3 μ L of the reaction mixture in sample buffer and run on 4-12% Bis-Tris gels (Invitrogen) by SDS-PAGE with MOPS as running buffer.

Flow cytometry

The binding of Rho-Ub $_2$ -Fab targeting mCD3 and FITC-labeled parental antibody (ThermoScientific, MA1-80640) to mCD3 positive EL4 cells was compared by staining 50,000 EL4 cells with 50 μ L of 1μ g/mL Rho-Ub $_2$ -Fab or FITC-labeled parental antibody for 30 minutes at 4 °C. Next, the cells were washed twice with PBS supplemented with 5% FCS and fluorescence intensity was measured on an LSR II flow cytometer (BD). A competitive binding assay was performed to assess the antigen binding of ubi-tagged antibody fragments and conjugates. Here, 50.000 EL4 cells per well were stained with 50 μ L of mCD3 targeting Fab-Ub, Fab-Ub2-Fab, or unlabeled parental antibody (ThermoScientific, MA1-80783), in increasing concentrations ranging from 0.01 to 1000 nM for 15 minutes at 4 °C. Next, the cells were washed with PBS supplemented with 5% FCS, followed by incubation with 1μ g/mL in 50 μ L of FITC-labeled parental antibody (ThermoScientific, MA1-80640) for 30 minutes at 4 °C. Cells were washed twice, and fluorescence intensity was measured by flow cytometry on an LSR II flow cytometer (BD).

In vitro serum stability assay

Human serum (Sigma-Aldrich, H4522) was diluted in PBS to 25% (v/v) and incubated at 37 °C for 15 minutes. Next, Rho-Ub $_2$ -Fab was added at a final concentration of 10 μM, and the mixture was incubated at 37 °C. The stability of Rho-Ub $_2$ -Fab over time was analyzed by quenching 5 μL of the reaction mixture in sample buffer supplemented with β-mercaptoethanol at specific time points (0, 0.5, 1, 2, 3, 6, and 24 hours). Samples were run on 4-12% Bis-Tris gels (Invitrogen) by SDS-PAGE with MOPS as running buffer. Serum stability of Rho-Ub $_2$ -Fab was visualized by in-gel fluorescence using Typhoon FLA 9500 imaging system (GE Life Sciences), followed by staining with InstantBlue Coomassie Protein Stain (abcam).

DUB cleavage assay

DUB cleavage of ubi-tagged Fab conjugates by OTUB1 was carried out using 5 μ M of either Rho-Ub₃-Fab and Fab-Ub₃-Fab and 1 μ M OTUB1 in PBS at 37 °C for 30-90 minutes.

The reaction efficiency was monitored by SDS-PAGE where samples were quenched at different time-point in sample buffer and run on 4-12% Bis-Tris gels (Invitrogen) by SDS-PAGE with MOPS as running buffer. Gels were stained using InstantBlue Coomassie Protein Stain (abcam) and imaged using Amersham600. Fluorescently labeled proteins were visualized by in-gel fluorescence using Typhoon FLA 9500 imaging system (GE Life Sciences) prior to staining with Coomassie.

Mice

All mice were purchased from Charles River Laboratories, France. All animal studies were approved by the local authority for the Ethical Evaluation of Animal Experiments and Animal Welfare (Instantie voor Dierenwelzijn Radboudumc). All mice were kept in accordance with federal and state policies on animal research and Annex III of the EU Directive (Directive 2010-63-EU). Female C57BL/6 WT and OTI (Tg(TcraTcrb)1100Mjb/Crl) between 8-12 weeks of age and 18-25 g body weight were used for *in vitro* and *in vivo* experiments. Mice were sacrificed by cervical dislocation.

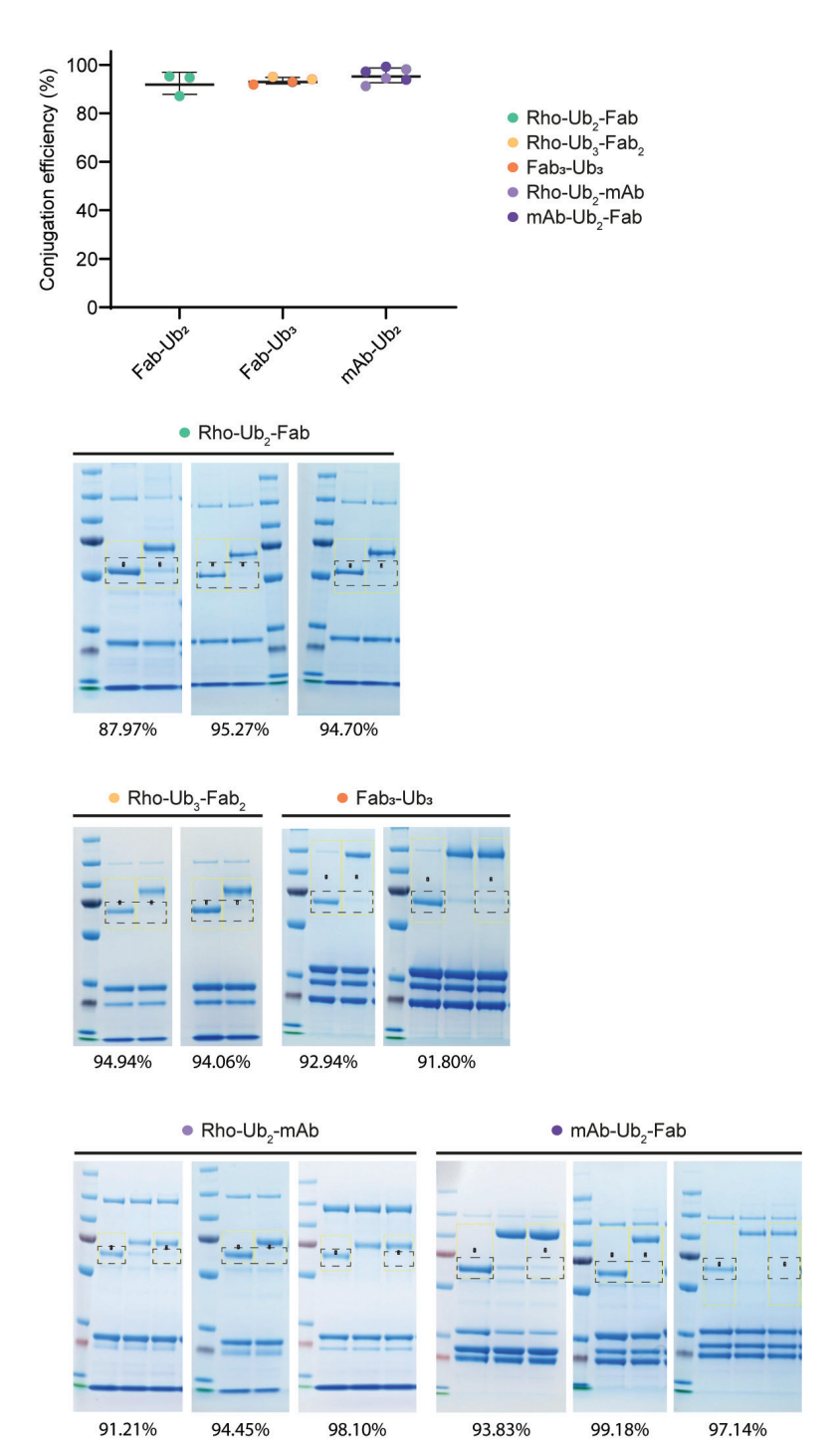
LDH assay

KPC3 or KPC3-Trp1 cells were irradiated with 6000 Rad to prevent proliferation, added to a 96-well plate, and incubated for 4 hours at 37 °C to facilitate adherence. Splenocytes were obtained from naïve C57BL/6 mice and CD8 T cells were purified using a CD8 enrichment kit (BD Biosciences, 558471). CD8 T cells were added in a 10:1 E:T ratio to the 96-well plate, followed by the addition of 0-1μg/mL of either the ubiconjugated TRP1xmCD3 bispecific or the unconjugated ubi-tagged TRP1 mAb + mCD3 Fab, and incubated for 48 hours. Tumor cell killing was assessed using the CyQUANT TM LDH cytotoxicity assay (ThermoFisher, C20301) following manufacturer's instructions. In parallel, CD8 T cells were stained with Zombie Aqua fixable viability dye (BioLegend, 423102), CD69 FITC (Invitrogen, 11-0691-82), and CD137 APC (BioLegend, 106110), and fluorescence was measured on the LSR II flow cytometer (BD) to determine T-cell activation. Fluorescence data were analyzed using FlowJo software.

Supplementary information

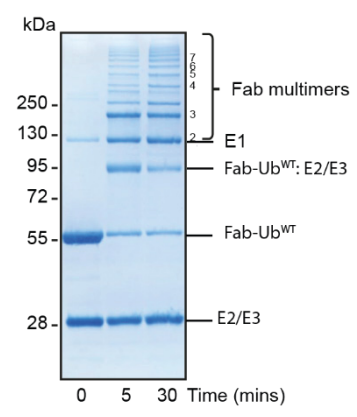


S1 Total chemical synthesis of Rho-Ubacc. The Ubacc lacking G75 and G76 (Ub Δ GG) was synthesized by linear solid-phase peptide synthesis (SPPS) on a trityl resin followed by coupling of diBoc-protected rhodamine (Rho) to the N-terminus. Next, removal of the protection groups (PG) and cleavage of Rho-Ubacc from resin was performed under strong acidic conditions. Reagents and conditions: a) N,N'-Boc-protected 5-carboxyrhodamine, PyBOP, DIPEA, NMP overnight at RT; b) TFA/H₂O/phenol/iPr₃SiH (90.5:5:2.5:2; v/v/v/v) for 3 h. at RT.

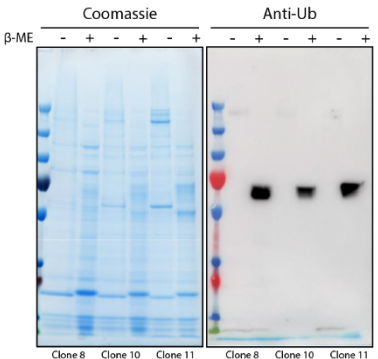


S2 The efficiency of ubi-tag conjugation reactions conducted in this study. Conjugation reactions involving ubi-tagged Fab fragments forming di-ubiquitin chains showed an average reaction efficiency

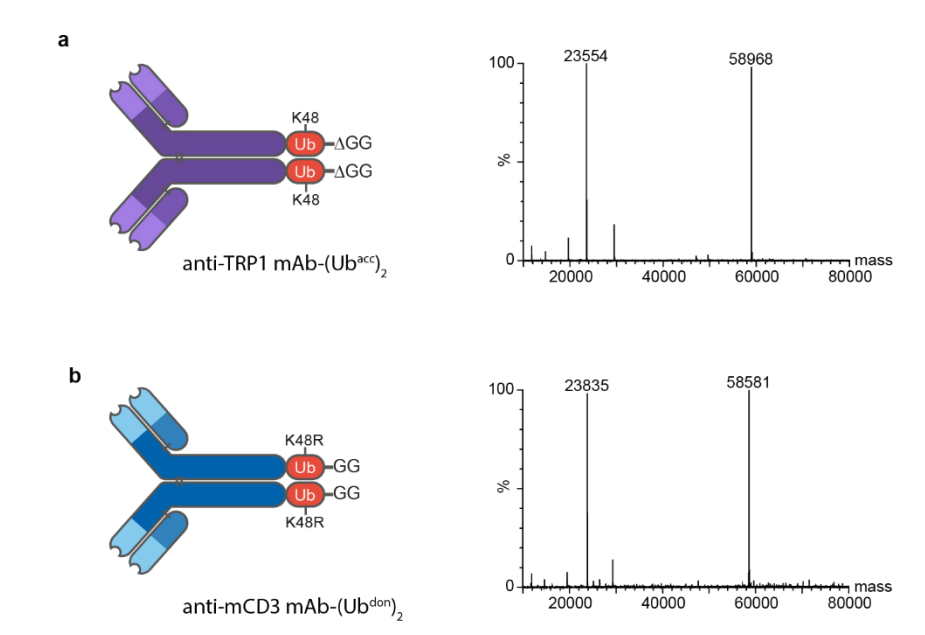
of 94.2% while conjugation reactions involving ubi-tagged Fabs forming tri-ubiquitin chains showed an average efficiency of 93.4%. Conjugation of ubi-tagged mAbs showed an average reaction efficiency of 95.7% within 60 mins. The conjugation reaction efficiency is calculated by quantifying the gel bands corresponding to the limiting reactant at the start and end of the reaction (indicated in the dashed boxes) and calculating the percentage of limiting reactant consumed.



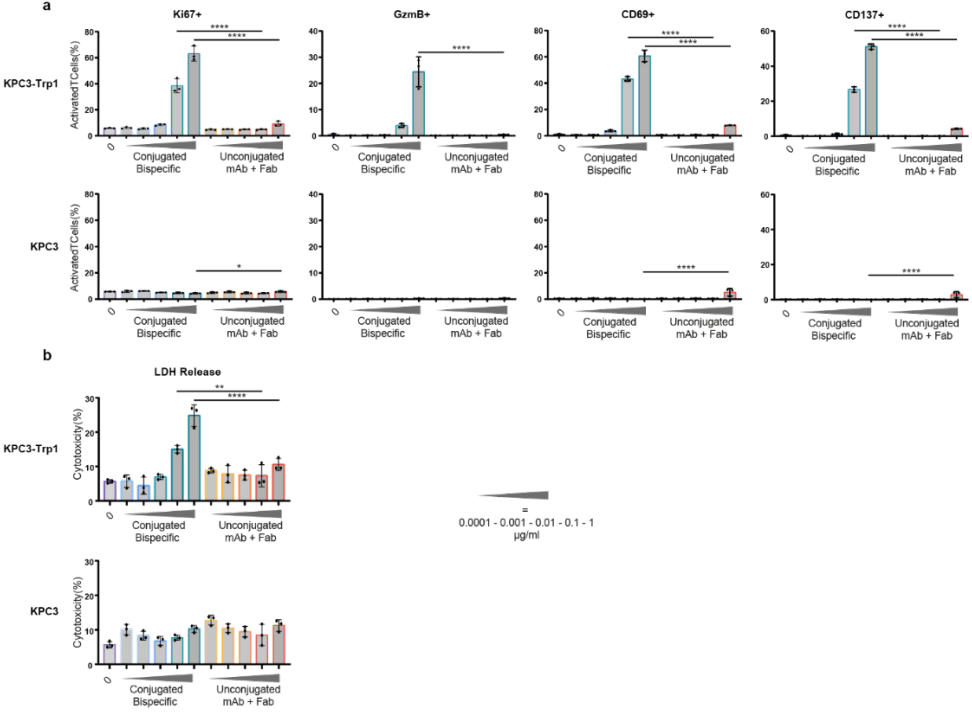
S3 Generation of multimeric Fab complexes using ubi-tag conjugation. Non-reducing SDS-PAGE stained with Coomassie staining of multimerization of Fab-Ub^{WT} showing the formation of multimers beyond the 11th order.



S4Validation of mAb-Ub producing hybridoma clones. SDS-PAGE analysis of hybridoma supernatants containing mAb-Ub in the absence or presence of β -mercaptoethanol, stained with Coomassie Blue and analyzed by western blot using an anti-Ub antibody.

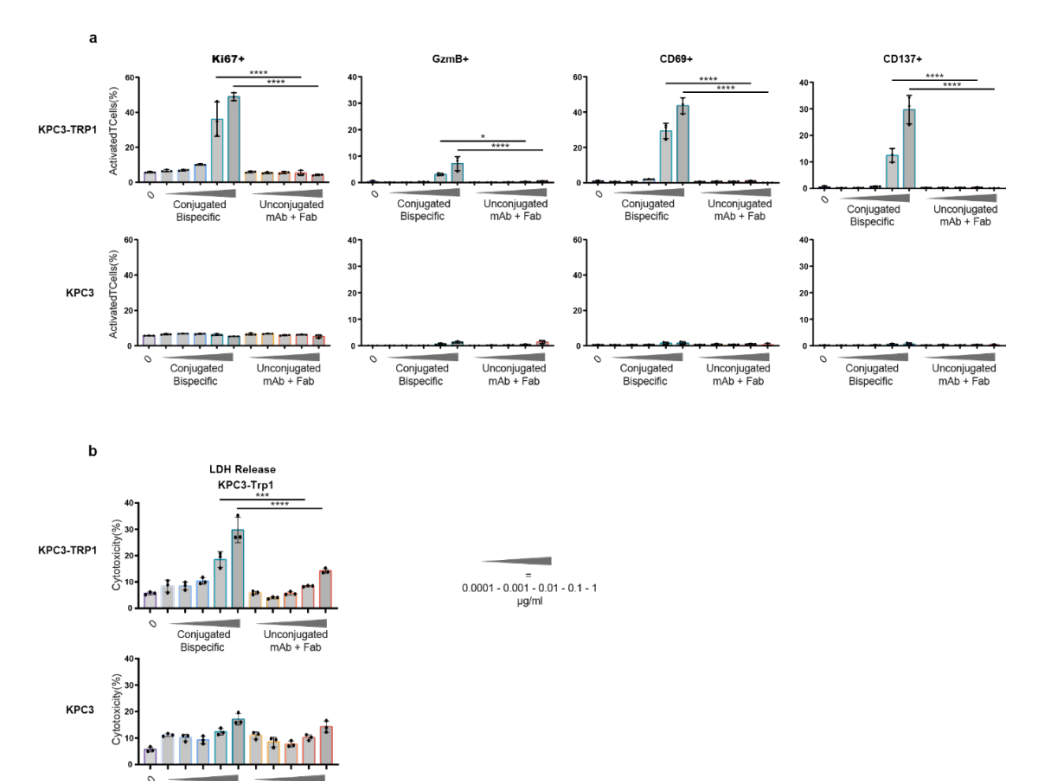


S5 LC-MS analysis showing the deconvoluted ESI-TOF mass spectra of (a) anti-TRP1 mAb- $(Ub^{acc})_2$ and (b) anti-mCD3 mAb- $(Ub^{don})_2$.

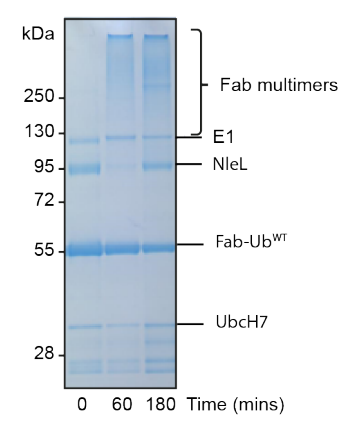


S6 In vitro T cell activation and tumor cell killing assay to validate the functionality of ubi-conjugated bispecific TRP1 mAb x mCD3 Fab antibody complex. CD8* T cells in the presence of KPC3-TRP1 cells

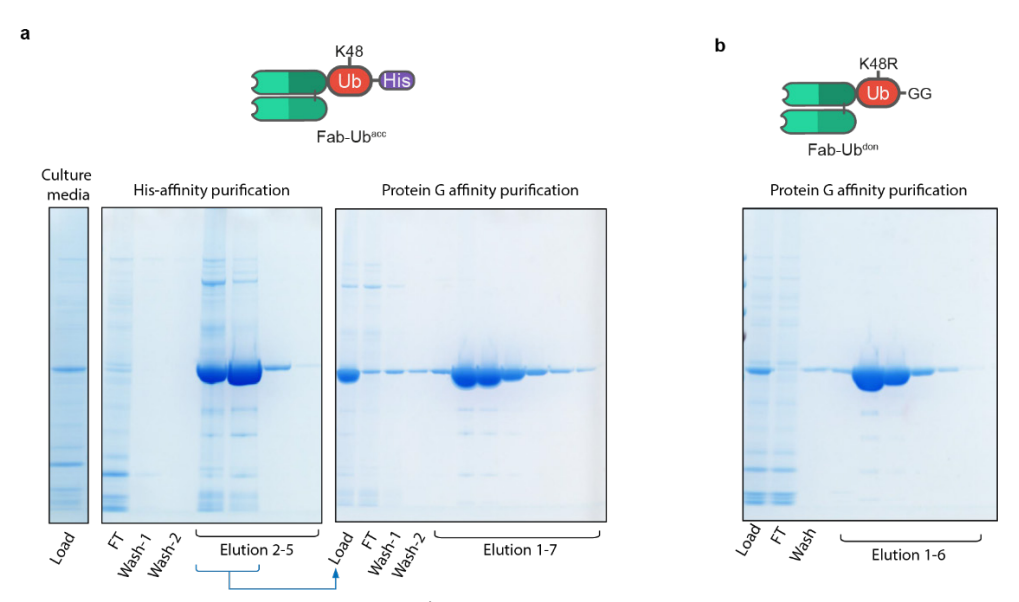
or control cells KPC1, were treated with increasing concentrations (0 – 1 μ g/mL) of the ubi-conjugated TRP1 mAb x mCD3 Fab bispecific or the unconjugated ubi-tagged TRP1 mAb and mCD3 Fab. (a) Surface expression of T cell activation markers Ki67, granzyme B, CD69 and CD137 were analyzed by flow cytometry. (b) Tumor cell killing was assessed using the CyQUANT TM LDH cytotoxicity assay. (a-b) Ordinary one-way Anova test was applied to the ubi-conjugated bispecific TRP1 mAb x mCD3 Fab vs. the unconjugated ubi-tagged TRP1 mAb and mCD3 Fab of the same concentration, showing only the significant values. All statistical values are shown in table S5. n=1 independent experiments, each condition performed in triplicates.



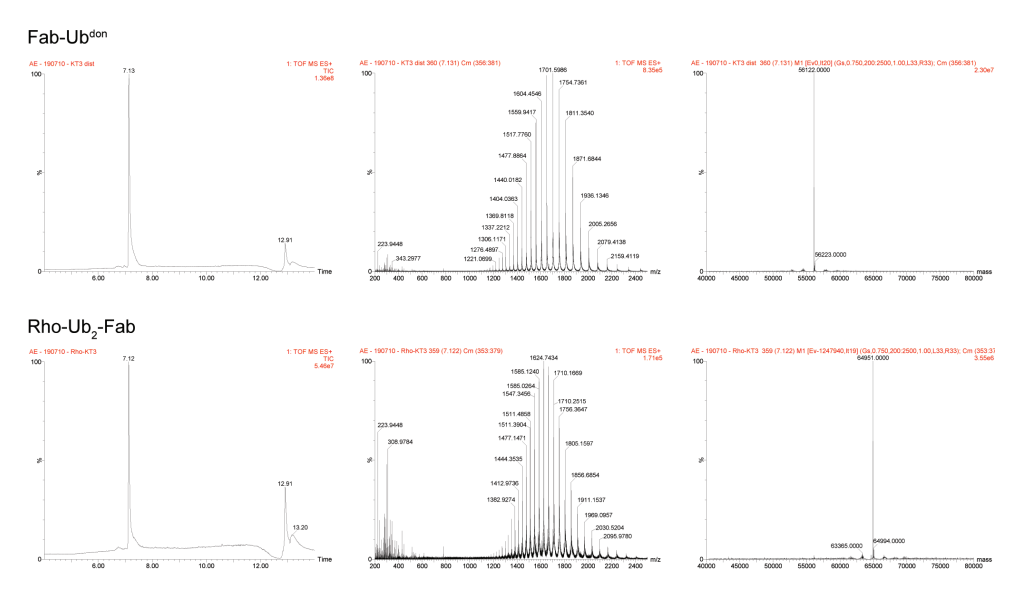
S7 In vitro T cell activation and tumor cell killing assay to validate the functionality of ubi-conjugated bispecific mCD3mAb x TRP1 Fab antibody complex. CD8+ T cells in the presence of KPC3-TRP1 cells or control cells KPC1, were treated with increasing concentrations (0 - 1 μ g/mL) of the ubi-conjugated bispecific mCD3 mAb x TRP1 Fab or the unconjugated ubi-tagged mCD3 mAb and TRP1 Fab. (a) Surface expression of T cell activation markers Ki67, granzyme B, CD69 and CD137 were analyzed by flow cytometry. (b) Tumor cell killing was assessed using the CyQUANT TM LDH cytotoxicity assay. (a-b) Ordinary one-way anova test was applied to the ubi-conjugated bispecific mCD3 mAb x TRP1 Fab vs. the unconjugated ubi-tagged mCD3 mAb and TRP1 Fab. of the same concentration, showing only the significant values. All statistical values are shown in table S5. n=3 independent experiments, each condition performed in triplicates.



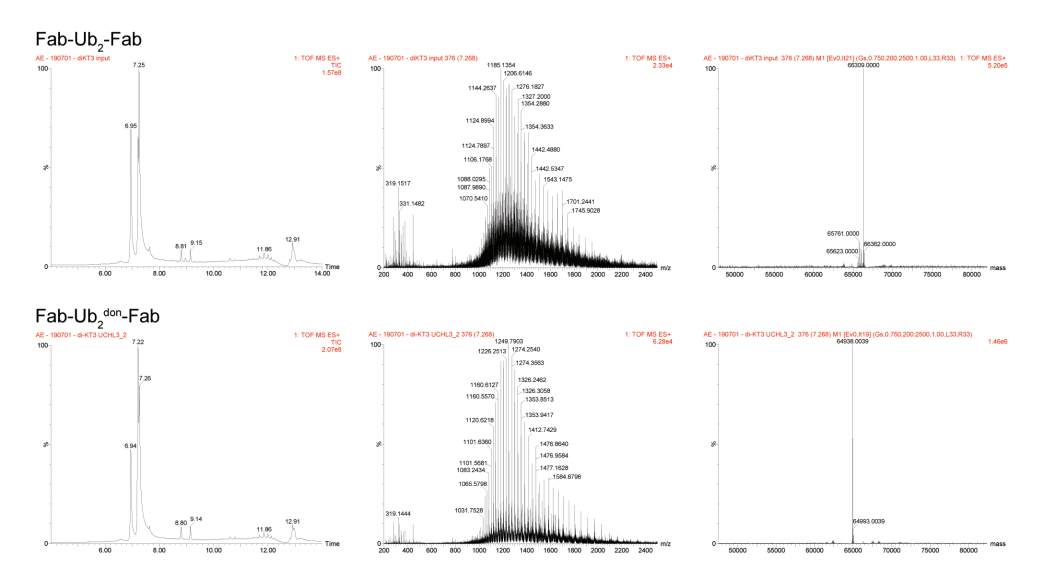
\$8 UbcH7 and NIeL for the generation of K6-linked ubi-tagged antibody multimers.



S9 Purification of Fab-Ub^{acc} and Fab-Ub^{don} from hybridoma culturing media. (a) Hybridoma cells secreting Fab-Ub^{acc} are cultured in presence of Ub-PA and Fab-Ub^{acc} is isolated from the culturing media by Ni-NTA followed by Protein G affinity purification to ensure the His-tag is present on all purified Fab-Ub^{acc}. (b) Hybridoma cells secreting Fab-Ub^{don} are cultured in absence of Ub-PA and Fab-Ub^{don} is purified from culturing media by Protein G affinity purification.



S10 LC-MS analysis of Fab-Ub^{don} **conjugation to Rho-Ub**^{acc} **forming Rho-Ub**₂-**Fab.** Total ion chromatograms (left), ESI-TOF spectra (middle) and deconvoluted ESI-TOF mass spectra (right).



S11 LC-MS analysis of the cleavage of His-tag from C-terminus of Fab-Ub₂-Fab by UCHL3. Total ion chromatograms (left), ESI-TOF spectra (middle) and deconvoluted ESI-TOF mass spectra (right).

Table S1 Rat IgG2A ubi-tagged Fab: donor and acceptor. Design HDR-template used to obtain the antimCD3 Fab-Ub^{don} and anti-mCD3 Fab-Ub^{acc}.

PCR4 TOPO	sequence
5'HA	CCTGGAACTCTGGAGCCCTGTCCAGCGGTGTGCACACCTTCCCAGCTGTCCTG-CAGTCTGGACTCTACACTCTCACCAGCTCAGTGACTGTACCCTCCAGCACCTGGTC-CAGCCAGGCCGTCACCTGCAACGTAGCCCACCCGGCCAGCACCAAGGTGGA-CAAGAAAATTGGTGAGAGAACAACCAGGGGATGAGGGCCACCAGGGAGGG
Linker - Ub ₁₋₇₆ -His _{10x} (acceptor)	TGCCAAGGGAATGCGGAGGCGGTGGATCTATGCAAATTTTCGTTAAGACTCT-GACAGGGAAGACTATTACACTGGAGGTTGAGCCATCAGATACGATTGAGAAT-GACAGGGAAGATACAGATACAGAAAGAAGGGTTCAAGGCCAACAAAGGCT-GATCTTCGCTGGGAAGCAACTGGAAGATGGCCGAACACTGAGCGATTATAACATA-CAAAAGGAGTCTACACTGCATTTGGTTCTGCGCCTTCGAGGCGGGCATCACCACCACCACCACCACCACCACCACCACCACCACC
Linker - Ub _{K48R} -His _{10x} (Donor)	TGCCAAGGGAATGCGGAGGCGGTGGATCTATGCAAATATTCGTAAAGACTCTGACC- GGGAAAACCATTACACTTGAAGTGGAGCCGTCAGACACGATTGAGAATGTTAAGGC- TAAGATTCAGGACAAGGAAGGTATCCCGCCAGACCAACAACGCCTGATCTTCGCCG- GACGACAATTGGAGGATGGTAGGACTTTGAGCGATTACAACATACAGAAAGAA
IRES Bsr polyA	CCGGTGAGCTCTCCCCCCCCCCCCTAACGTTACTGGCCGAAGCCGCTTGGAATAAGGCCGGTGTGCGTTTGTCTATATGTTATTTTCCACCATATTGCCGAATAAGGCCGGTGTGCGTTTGTCTATATGTTATTTTCCACCATATTGCCGTCTTTTTGGCAATGTGAGGGCCCGGAAACCTGGCCCTGTCTTCTTGACGAGGCATTCCTAGGGGGTCTTTCCCCTCTCGCCAAAGGAATGCAAGGTCTGTTGAATGCGTGGAAGCAAGGAAGAACAACGTCTGGAAGCACCCCACCTGGCGAAAGCAACCACCCAGTGCGGCAAAAGCCACCCAGTGAAAAGCCACCTGGCAAAAGCCACCCAGTGCTCCAAAAGCCACCGTGTATAAAGAATACACCTGCAAAAGCCACCCAGTGCCAAAAGCCACCGTGTATTCAACAAGGGGCTGAAAGGCCACCAAGCCCCAGTGCCAACCCCAGTGCTATTCAACAAGGGGCTGAAAGGATGCCCAAAGGCCCCAATTGTATGGGATCTGAATCAACAAGGGGCCTCAAAGCCCAATTGTATGGGATCTGAACAAGGGCCCCCGAACCACGGGGACCCCAGAAGGTACCCCATTTGTATGGGATCTGAACAAAAAACCGATGATAATTCAACAAGGGCCCCCGAACCACGGGGACGTGGTTTTCCTTTGAAAAAAACACGATGATAATTAAAAAAACACGATGATAAAAAACCGATGATAAAAAACACGATGATAAAAAAACACGATGATAAAAAAACACGATGATAAAAAAACACGATGATAAAAAAACACGATGATAAAAAAACACGATGATAAAAAAACACGATGATAAAAAAAA

3'HA	GGTAAGTCACTAGGACTATTACTCCAGCCCCAGATTCAAAAAATATCCTCAGAG-
	GCCCATGTTAGAGGATGACACAGCTATTGACCTATTTCTACCTTTCTTCATC-
	TACAGGCTCAGAAGTATCATCTGTCTTCATCTTCCCCCCAAAGACCAAAGATGT-
	GCTCACCATCACTCTGACTCCTAAGGTCACGTGTGTTGTGGTAGACATTAGC-
	CAGAATGATCCCGAGGTCCGGTTCAGCTGGTTTATAGATGACGTGGAAGTCCA-
	CACAGCTCAGACTCATGCCCCGGAGAAGCAGTCCAACAGCACTTTACGCTCAGT-
	CAGTGAACTCCCCATCGTGCACCGGGACTGGCTCAATGGCAAGACGTTCAAATG-
	CAAAGTCAACAGTGGAGCATTCCCTGCCCCCATCGAGAAAAGCATCTCCAAACCC-
	GAAGGTGGGAGCAGCAGGTGTGTGTGTAGAAGCTGCAGTAGGCCATAGA-
	CAGAGCTTGACTTAACTAGACTTAAGGGCGAATTCGCGGCCGCGCGGCCGC

Table S2 mlgG2a Hinge targeted to mlgG2a-Fc silent – ubiquitin.

Mus musculus strain 129S1/SvImJ chromosome 12 genomic scaffold, GRCm38.p4 alternate locus group 129S1/SvImJ 129S1/SVIMJ MMCHR12 CTG1

Sequence ID: NT_114985.3 Length: 1714434 Number of Matches: 7

CCAGGGACAAAGTCCCTGGTTTGGTGCCTTTCTCCTTCAAACTTGAGTAACCCCCAGCCTTCTCTCTGCAGAGGCCCAGAGGGCCCACAATCAAGCCCTGTCCTCCATGCAAATGCCCAGGTAAGTCACTAGACCAGAGCTCCACTCCCGGGAGAATGGTAAGTGCTGTAAACATCCCTGCACTAGAGGATAAGCCATGTACAGATCCATTTCCATCTCT(85) TGGAGGACAGGGCTTGATTG TGG

Genomic Sequence and annotated base pair sequence of mlgG2a constant domains. The genomic annotated basepair sequence and of the lgH locus of murine lgG2a located on chromosome 12 are given. The Hinge region is indicated (grey highlight) with splice acceptor and donor sites (underlined, cursive). The targeted protospacer adjacent motifs (PAMs) for gRNA-6 (yellow, underlined) and gRNA-2 (red. underlined) are indicated.

PCR4 TOPO	sequence
5'HA mlgG2a	ACTAGTGATCCCTGTCCAGTGGTGTGCACACCTTCCCAGCTGTCCTG-CAGTCTGACCTCTACACCCTCAGCAGCTCAGTGACTGTAACCTCGAG-CAGTCTGACCTCAGCAGCCCAGCC
Fc silent mlgG2a	GCCCCAAATGCCGCCGGTGGTCCTAGCGTCTTCATCTTCCCCCCCAAGATTA- AGGATGTGCTGATGATTTCATTGAGCCCAATTGTCACATGTGTGGTCGTGGATGT- GTCAGAGGATGACCCTGACGTGCAAATATCTTGGTTTGTAAATAACGTAGAGGTG- CATACCGCTCAGACTCAGACTCACCGGGAGGACTATGCCAGCACTCTCAGGGTG- GTCTCCGCACTTCCAATTCAGCACCAGGACTGGATGTCCGGCAAAGAGTTCAAGTG- TAAAGTCAATAACAAGGATTTGCCCGCACCAATAGAACGGACCATCTCTAAACCTA- AAGGGAGTGTACGCGCCCCACAGGTTTACGTGCTGCCCCCACCCGAGGAGGAAAT- GACCAAAAAGCAGGTGACACTCACCTGCATGGTTACCGATTTTATGCCCGAAGA- CATATATGTTGAGTGGACTCACACGGGAAGACCGAGCTGAATTATAAAAATAC- CGAACCCGTTTTGGACTCAGATGGCTCATACTTCATGTACTCCAAACTCCGGG- TAGAGAAAAAGAACTGGGTTGAAAGAACAGCTACTCATGCAGCGTGGTGCATGAG- GGGCTCCACAATCATCATACCACCAAGTCTTTCTCACGGACACCTGGGAAA

Linker - Ub	GGCGGGGGGATCCGGGGGAGGCGGAAGTGGGGGCGGAGGCTCCATG-
(acceptor)	CAAATTTTCGTTAAGACTCTGACAGGGAAGACTATTACACTGGAGGTTGAGCCAT-CAGATACGATTGAGAATGTCAAGGCAAAGATACAGGACAAAGAAGGGATACCCCC-GGACCAACAAAGGCTGATCTTCGCTGGGAAGCAACTGGAAGATGGCCGAACACT-GAGCGATTATAACATACAAAAGGAGTCTACACTGCATTTGGTTCTGCGCCTTC
IRES Bsr polyA	TCCCTCCCCCCCCTAACGTTACTGGCCGAAGCCGCTTGGAATAAGGC-CGGTGTGCGTTTGTCTATATGTTATTTTCCACCATATTGCCGTCTTTTG-GCAATGTGAGGGCCCGGAAACCTGGCCCTGTCTTCTTGACGAGCATTCCTAGGGGTCTTTTCCCCTCTCGCCAAAGGAATGCAAGGTCTGTTGAATGTCGT-GAAGGAAGCAGCTCCTCTGGCAAAGGAATGCAAGGTCTGTTGAATGTCGT-GAAGGAAGCAGCACCCCCCCCCC
3'HA mIgG2a	GGTAAGTCACTAGACCAGAGCTCCACTCCCGGGAGAATGGTAAGTGCTGTAAA- CATCCCTGCACTAGAGGATAAGCCATGTACAGATCCATTTCCATCTCCTCAT- CAGCACCTAACCTCTTGGGTGGACCATCCGTCTTCATCTTCCCTCCAAAGAT- CAAGGATGTACTCATGATCTCCCTGAGCCCCATAGTCACATGTGTGGTGGTGGAAG- GTGAGCGAGGATGACCCAGATGTCCAGATCAGCTGGTTTTGTGAACAACGTGGAAG- TACACACAGCTCAGACCACAAACCCATAGAGAGGATTACAACAGTACTCTCCGGGTG- GTCAGTGCCCTCCCCATCCAGCACCAGGACTGGATGAGTGGCAAGGAGTTCAAAT- GCAAGGTCAACAACAAAGACCTCCCAGCCCCATCGAGAGAACCATCT- CAAAACCCAAAGGTGAGAGCTGCAGCCTGACTGCATGGGGGCTGGGATGGCCATA- AGGATAAAGGTCTGTGTGGACAGC GCGGCCGC

Table S3 Rat IgG2a intron targeted to mIgG1-ubiquitin. Isotype donor constructs for HDR introducing synthetic exon. Table displays sequences of each feature of donor constructs used to change the isotype of rat IgG2a hybridomas to mIgG1 fused to Ubiquitin with a HIS tag. The gRNA-ISO and sequences of 5' HA, IRES-Bsr-PolyA and 3' HA of the HDR plasmid are previous published³⁸.

5 111 y 11125 251 1 51 y 1 1	Someone
	Sequence
5'HA rIgG2a	AGAAAGATCTGAGTAGAACCAAGGTAAAAAGTGTGGGTAAAAACACATGTTCA- CAGGCCTGGCTGACATGATGCTGGGCACGTATGAGGCCAAAGTCAAGAGGGCAGT- GTAAGGGCCAGAAGTGAATCCTGACCCAAGAAATAGAGAGTGCTAAACCTACG- TAGATCGAAGCCAACTAAAAAGACAAGCTACAAACGAAGCTAAGGCCAGA- GATCTTGGACTGTGAAGAGTTCAGAGACCTAGGATCAGGAACCATTAGTAA- CAGGCCAAGGAAGATAGAAGCTGCCTAGGACTTGGCAACATGGTTG- GACTGGAAAAGAAAGGAGGAGACAGAAGACAGGAGAGATATGGCCAACTT- GATTTTGGGCTTCACTGTTGTCCATACTGTTGCAGCCATATGGCCCACAGATAA- CAGGTTTAGCCGAGGAACACAGATACCCACATTTGGACAATGGTGGGGGAACA- CAGATACCCATACTACAGGGCTCTTTAGGGCATTTCCTGAAAGTGTACTAG- GAGTGGGACTGGGCTCAAAGGGATTAGGTTGGCCTGGTGAGGCT- GACATTGGCAAGCCCAATGGTTGGCCTCCTCCATGT
Splice Acceptor	GCTAGCgatcgcaggcgcaatcttcgcatttcttttttccag
mlgG1	CAAAGACCACCACCTTCTGTGTACCCACTCGCACCAGGCAGCGCCGCTCAAACCCAACAGTATGGTGACCTTGGGGTGTCTTGTGAAGGGCTACTTTCCCGAGCCCGTTACCGTCACCTGGAACTCCGGGTTCTCTCAAGCGGCGTTCACACCTTCCCCGCCGTACTGCAATCAGACTCCTATACCCTGTCTTCCAGCGGTCACTGTACCCAGTTCCACCTTGCCAGTTCCACCTTGCCAGTTCCACCTTGCCAGTTCCACCTTGCCAGTTCCACCTTGCCCAGTTCCACCTTGCCCAGTTCCACCTTGCCCAGTTCCACCTTGCCCAGTTGAAACAGTGCACAAAAAAAA
Linker - Ub _{K48R} - His _{10x}	CGTACGGGAGGTGGCGGTTCCGGGGGAGGTGGATCTGGAGGGGGCGGAAGTG-GCGGTGGTGGATCAATGCAAATATTCGTAAAGACTCTGACCGGGAAAACCATTA-CACTTGAAGTGGAGCCGTCAGACACGATTGAGAATGTTAAGGCTAAGATTCAG-
(Donor)	GACAAGGAAGGTATCCCGCCAGACCAACAACGCCTGATCTTCGCCGGACGA- CAATTGGAGGATGGTAGGACTTTGAGCGATTACAACATACAGAAAGAA

IDEC Daniela	GCCCCTCTCCCTCCCCCCCCCTAACGTTACTGGCCGAAGCCGCTTG-
IRES Bsr polyA	GAATAAGGCCGGTGTGCGTTTGTCTATATGTTATTTTCCACCATATTGCC-
	GTCTTTTGGCAATGTGAGGGCCCGGAAACCTGGCCCTGTCTTCTTGACGAG-
	CATTCCTAGGGGTCTTTCCCCTCTCGCCAAAGGAATGCAAGGTCTGTTGAAT-
	GTCGTGAAGGAAGCAGTTCCTCTGGAAGCTTCTTGAAGACAAACAA
	TAGCGACCCTTTGCAGGCAGCGGAACCCCCCACCTGGCGACAGGTGCCTCTGC-
	GGCCAAAAGCCACGTGTATAAGATACACCTGCAAAGGCGGCACAACCCCAGT-
	GCCACGTTGTGAGTTGGATAGTTGTGGAAAGAGTCAAATGGCTCTCCT-
	CAAGCGTATTCAACAAGGGGCTGAAGGATGCCCAGAAGGTACCCCATTG-
	TATGGGATCTGATCTGGGGCCTCGGTGCACATGCTTTACATGTGTTTAGTC-
	GAGGTTAAAAAAACGTCTAGGCCCCCCGAACCACGGGGACGTGGTTTTCCTTT-
	GAAAAACACGATGATAATATGGCCACAGAATTCGCCACCATGGCCAAGCCTTT-
	GTCTCAAGAAGAATCCACCCTCATTGAAAGAGCAACGGCTACAATCAACAG-
	CATCCCCATCTCTGAAGACTACAGCGTCGCCAGCGCAGCTCTCTCT
	GGCCGCATCTTCACTGGTGTCAATGTATATCATTTTACTGGGGGACCTTGTG-
	CAGAACTCGTGGTGCTGGGCACTGCTGCTGCTGCGGCAGCTGGCAACCTGACTT-
	GTATCGTCGCGATCGGAAATGAGAACAGGGGCATCTTGAGCCCCTGCGGACG-
	GTGCCGACAGGTGCTTCTCGATCTGCATCCTGGGATCAAAGCCATAGTGAAGGA-
	CAGTGATGGACAGCCGACGGCAGTTGGGATTCGTGAATTGCTGCCCTCTGGT-
	TATGTGTGGGAGGGCTAAGTACTAGTCGAGTGTGCCTTCTAGTTGCCAGCCA
	GTTGTTTGCCCCTCCCCCGTGCCTTCCTTGACCCTGGAAGGTGCCACTCCCACT-
	GTCCTTTCCTAATAAAATGAGGAAATTGCATCGCATTGTCTGAGTAGGTGCCACTC
	TATTCTGGGGGGTGGGGCAGGACAGCAAGGGGGAGGATTGGGAAGACAATAG-
	CAGGCATGCTGGGGATGCGGTGGGCTCTATGGAGATCT
3'HA rlgG2a	TGTACAACTTGGGGAGGGTACAAAATGGAGGACTTGTAGGAGCTTGGGTC-
	CAGACCTGTCAGACAAAATGATCACGCATACTTATTCTTGTAGCTGAAACAA-
	CAGCCCCATCTGTCTATCCACTGGCTCCTGGAACTGCTCTCAAAAGTAACTC-
	CATGGTGACCCTGGGATGCCTGGTCAAGGGCTATTTCCCTGAGCCAGTCACCGT-
	GACCTGGAACTCTGGAGCCCTGTCCAGCGGTGTGCACACCTTCCCAGCTGTCCT-
	GCAGTCTGGACTCTACACTCTCACCAGCTCAGTGACTGTACCCTCCAGCACCTG-
	GTCCAGCCAGGCCGTCACCTGCAACGTAGCCCACCCGGCCAGCAGCACCAAGGTG-
	GACAAGAAATTGGTGAGAGAACAACCAGGGGATGAGGGGCTCACTAGAG-
	GTGAGGATAAGGCATTAGATTGCCTACACCAACCAGGGTGGGCAGACATCAC-
	CAGGGAGGGGCCTCAGCCCAGGAGACCAAAAATTCTCCTTTGTCTCCCTTCTGGA-
	GATTTCTATGTCCTTTACACCCATTTATTAATATTCT

Table S4 Recombinant ubitagged Fab fragments produced by Genscript. Table displays protein sequence of recombinant constructs used. Clone TA99 is directed against Tryp-1 and clone 145-2C11 is against mCD3.

	Sequence
IgH chain TA99	MGWSCIILFLVATATGVHSEVQLQQSGAELVRPGALVKLSCKTSGFNIKDY-FLHWVRQRPDQGLEWIGWINPDNGNTVYDPKFQGTASLTADTSSNTVYLQLS-GLTSEDTAVYFCTRRDYTYEKAALDYWGQGTTVTVSTAKTTAPSVYPLAPVC-GDTTGSSVTLGCLVKGYFPEPVTLTWNSGSLSSGVHTFPAVLQSDLYTLSSS-VTVTSSTWPSQSITCNVAHPASSTKVDKKI
Linker-ubi	GGGGSGGGGGGGGMQIFVKTLTGKTITLEVEPSDTIENVKAKIQDKEGIP- PDQQRLIFAGKQLEDGRTLSDYNIQKESTLHLVLRLR
His-tag	ннинин*

IgL chain TA99	MGWSCIILFLVATATGVHSDIQMSQSPASLSASVGETVTITCRASGNIYNYL- AWYQQKQGKSPHLLVYDAKTLADGVPSRFSGSGSGTQYSLKISSLQTEDS- GNYYCQHFWSLPFTFGSGTKLEIKRADAAPTVSIFPPSSEQLTSGGASVVC- FLNNFYPKDINVKWKIDGSERQNGVLNSWTDQDSKDSTYSMSSTLTLTKDEY- ERHNSYTCEATHKTSTSPIVKSFNRNEC*
IgH chain 145-2C11	MGWSCIILFLVATATGVHSEVQLVESGGGLVQPGKSLKLSCEASGFTFS-GYGMHWVRQAPGRGLESVAYITSSSINIKYADAVKGRFTVSRDNAKNLL-FLQMNILKSEDTAMYYCARFDWDKNYWGQGTMVTVSSAKTTAPSVYPLAPVC-GDTTGSSVTLGCLVKGYFPEPVTLTWNSGSLSSGVHTFPAVLQSDLYTLSSS-VTVTSSTWPSQSITCNVAHPASSTKVDKKI
Linker-Ub ^{don}	GGGGSGGGSGGGSMQIFVKTLTGKTITLEVEPSDTIENVKAKIQDKEGIP- PDQQRLIFAGRQLEDGRTLSDYNIQKESTLHLVLRLRGG
His-tag	ннинин*
IgL chain 145-2C11	MGWSCIILFLVATATGVHSDIQMTQSPSSLPASLGDRVTINCQASQDISNYL- NWYQQKPGKAPKLLIYYTNKLADGVPSRFSGSGSGRDSSFTISSLESEDIG- SYYCQQYYNYPWTFGPGTKLEIKRADAAPTVSIFPPSSEQLTSGGASVVC- FLNNFYPKDINVKWKIDGSERQNGVLNSWTDQDSKDSTYSMSSTLTLTKDEY- ERHNSYTCEATHKTSTSPIVKSFNRNEC

Table S5 Statistics for figure 3 and supplemental figure 7 and 8. ****P<0.0001, ***P<0.001, **P<0.001, **P<0.005 and ns= non-significant in a One-way ANOVA followed by Tukey post-hoc test.

	_	•	•		
	KPC3-TRP1 cells				
	Conjugated TRP1	mAb x mCD3Fab vs	s. the unconjugated	TRP1mAb and mC	D3Fab
Conc. (µg/mL)	0.0001	0.001	0.01	0.1	1
Ki67	0.9997, ns	>0.9999, ns	0.7607, ns	<0.0001, ****	<0.0001, ****
GzmB	>0.9999, ns	>0.9999, ns	>0.9999, ns	0.2771, ns	<0.0001, ****
CD69	>0.9999, ns	>0.9999, ns	0.331, ns	<0.0001, ****	<0.0001, ****
4-1BB	>0.9999, ns	>0.9999, ns	0.8061, ns	<0.0001, ****	<0.0001, ****
LDH	0.7266, ns	0.6012, ns	>0.9999, ns	0.0037, **	<0.0001, ****

	KPC3 cells Conjugated TRP1mAb x mCD3Fab vs. the unconjugated TRP1mAb and mCD3Fab				
Conc. (µg/mL)	0.0001	0.001	0.01	0.1	1
Ki67	0.2068, ns	0.8187, ns	0.9917, ns	0.9991, ns	0.0337, *
GzmB	>0.9999, ns	>0.9999, ns	>0.9999, ns	0.9991, ns	0.9852, ns
CD69	>0.9999, ns	>0.9999, ns	>0.9999, ns	>0.9999, ns	<0.0001, ****
4-1BB	>0.9999, ns	>0.9999, ns	>0.9999, ns	>0.9999, ns	<0.0001, ****
LDH	0.5391, ns	0.7981, ns	0.5747, ns	0.9998, ns	0.9991, ns

	KPC3-TRP1 cells						
	Conjugated mCD3mAb x TRP1Fab vs. the unconjugated mCD3mAb and TRP1Fab						
Conc. (µg/mL)	0.0001	0.0001 0.001 0.01 1					
Ki67	>0.9999, ns	0.9999, ns	0.7703, ns	<0.0001, ****	<0.0001, ****		
GzmB	>0.9999, ns	>0.9999, ns	>0.9999, ns	0.0209, *	<0.0001, ****		
CD69	>0.9999, ns	>0.9999, ns	0.9987, ns	<0.0001, ****	<0.0001, ****		

4-1BB	>0.9999, ns	>0.9999, ns	>0.9999, ns	<0.0001, ****	<0.0001, ****
LDH	0.8808, ns	0.2477, ns	0.2104, ns	0.0002, ***	<0.0001, ****

	KPC3 cells				
	Conjugated mCD3mAb x TRP1Fab vs. the unconjugated mCD3mAb and TRP1Fab				
Conc. (µg/mL)	0.0001	0.001	0.01	0.1	1
Ki67	>0.9999, ns	>0.9999, ns	0.3557, ns	>0.9999, ns	>0.9999, ns
GzmB	>0.9999, ns	>0.9999, ns	0.9997, ns	0.9447, ns	>0.9999, ns
CD69	>0.9999, ns	0.9878, ns	>0.9999, ns	0.9183, ns	0.1305, ns
4-1BB	>0.9999, ns	0.9862, ns	>0.9999, ns	0.9966, ns	0.3262, ns
LDH	>0.9999, ns	0.9439, ns	0.9547, ns	0.7421, ns	0.4074, ns

References

- 1. Sun, M. M. C. *et al.* Reduction-alkylation strategies for the modification of specific monoclonal antibody bisulfides. *Bioconjug Chem* **16**, 1282–1290 (2005).
- 2. Junutula, J. R. *et al.* Site-specific conjugation of a cytotoxic drug to an antibody improves the therapeutic index. *Nature Biotechnology 2008 26:8* **26**, 925–932 (2008).
- 3. Yamada, K. & Ito, Y. Recent Chemical Approaches for Site-Specific Conjugation of Native Antibodies: Technologies toward Next-Generation Antibody–Drug Conjugates. *ChemBioChem* **20**, 2729–2737 (2019).
- 4. Wang, L., Amphlett, G., Blättler, W. A., Lambert, J. M. & Zhang, W. Structural characterization of the maytansinoid-monoclonal antibody immunoconjugate, huN901-DM1, by mass spectrometry. *Protein Sci* **14**, 2436–2446 (2005).
- 5. Strop, P. *et al.* Location Matters: Site of Conjugation Modulates Stability and Pharmacokinetics of Antibody Drug Conjugates. *Chem Biol* **20**, 161–167 (2013).
- 6. Shen, B. Q. *et al.* Conjugation site modulates the in vivo stability and therapeutic activity of antibody-drug conjugates. *Nature Biotechnology 2012 30:2* **30**, 184–189 (2012).
- 7. Agarwal, P. & Bertozzi, C. R. Site-specific antibody-drug conjugates: The nexus of bioorthogonal chemistry, protein engineering, and drug development. *Bioconjug Chem* **26**, 176–192 (2015).
- 8. Axup, J. Y. *et al.* Synthesis of site-specific antibody-drug conjugates using unnatural amino acids. *Proc Natl Acad Sci U S A* **109**, 16101–16106 (2012).
- 9. Oller-Salvia, B., Kym, G. & Chin, J. W. Rapid and Efficient Generation of Stable Antibody—Drug Conjugates via an Encoded Cyclopropene and an Inverse-Electron-Demand Diels—Alder Reaction. *Angewandte Chemie International Edition* **57**, 2831—2834 (2018).

- 10. Kim, C. H. *et al.* Synthesis of bispecific antibodies using genetically encoded unnatural amino acids. *J Am Chem Soc* **134**, 9918–9921 (2012).
- 11. Hofer, T., Skeffington, L. R., Chapman, C. M. & Rader, C. Molecularly defined antibody conjugation through a selenocysteine interface. *Biochemistry* **48**, 12047–12057 (2009).
- 12. Zimmerman, E. S. *et al.* Production of site-specific antibody-drug conjugates using optimized non-natural amino acids in a cell-free expression system. *Bioconjug Chem* **25**, 351–361 (2014).
- 13. van Geel, R. *et al.* Chemoenzymatic Conjugation of Toxic Payloads to the Globally Conserved N-Glycan of Native mAbs Provides Homogeneous and Highly Efficacious Antibody-Drug Conjugates. *Bioconjug Chem* **26**, 2233–2242 (2015).
- 14. Ruhe, L., Ickert, S., Beck, S. & Linscheid, M. W. A new strategy for metal labeling of glycan structures in antibodies. *Anal Bioanal Chem* **410**, 21–25 (2018).
- 15. Toftevall, H., Nyhlén, H., Olsson, F. & Sjögren, J. Antibody Conjugations via Glycosyl Remodeling. *Methods in Molecular Biology* **2078**, 131–145 (2020).
- 16. Strop, P. Versatility of microbial transglutaminase. *Bioconjug Chem* **25**, 855–862 (2014).
- 17. Drake, P. M. *et al.* Aldehyde tag coupled with HIPS chemistry enables the production of ADCs conjugated site-specifically to different antibody regions with distinct in vivo efficacy and PK outcomes. *Bioconjug Chem* **25**, 1331–1341 (2014).
- 18. Zang, B. *et al.* Freezing-assisted synthesis of covalent C–C linked bivalent and bispecific nanobodies. *Org Biomol Chem* **17**, 257–263 (2019).
- 19. Beerli, R. R., Hell, T., Merkel, A. S. & Grawunder, U. Sortase Enzyme-Mediated Generation of Site-Specifically Conjugated Antibody Drug Conjugates with High In Vitro and In Vivo Potency. *PLoS One* **10**, e0131177 (2015).
- 20. Swee, L. K. *et al.* Sortase-mediated modification of aDEC205 affords optimization of antigen presentation and immunization against a set of viral epitopes. *Proc Natl Acad Sci U S A* **110**, 1428–1433 (2013).
- 21. Bridoux, J. *et al.* Anti-Human PD-L1 Nanobody for Immuno-PET Imaging: Validation of a Conjugation Strategy for Clinical Translation. *Biomolecules 2020, Vol. 10, Page 1388* **10**, 1388 (2020).
- 22. Morgan, H. E., Turnbull, W. B. & Webb, M. E. Challenges in the use of sortase and other peptide ligases for site-specific protein modification. *Chem Soc Rev* **51**, 4121–4145 (2022).
- 23. Bartels, L., Ploegh, H. L., Spits, H. & Wagner, K. Preparation of bispecific antibody-protein adducts by site-specific chemo-enzymatic conjugation. *Methods* **154**, 93–101 (2019).

- 24. Wagner, K. *et al.* Bispecific antibody generated with sortase and click chemistry has broad antiinfluenza virus activity. *Proc Natl Acad Sci U S A* **111**, 16820–16825 (2014).
- 25. Hershko, A. & Ciechanover, A. The ubiquitin system. *Annu Rev Biochem* **67**, 425–479 (1998).
- 26. Komander, D. & Rape, M. The ubiquitin code. *Annu Rev Biochem* **81**, 203–229 (2012).
- 27. Yau, R. & Rape, M. The increasing complexity of the ubiquitin code. *Nature Cell Biology 2016 18:6* **18**, 579–586 (2016).
- 28. Damgaard, R. B. The ubiquitin system: from cell signalling to disease biology and new therapeutic opportunities. *Cell Death & Differentiation 2021 28:2* **28**, 423–426 (2021).
- 29. Schulman, B. A. & Wade Harper, J. Ubiquitin-like protein activation by E1 enzymes: the apex for downstream signalling pathways. *Nature Reviews Molecular Cell Biology 2009 10:5* **10**, 319–331 (2009).
- 30. Ye, Y. & Rape, M. Building ubiquitin chains: E2 enzymes at work. *Nature Reviews Molecular Cell Biology 2009 10:11* **10**, 755–764 (2009).
- 31. Buetow, L. & Huang, D. T. Structural insights into the catalysis and regulation of E3 ubiquitin ligases. *Nature Reviews Molecular Cell Biology 2016 17:10* **17**, 626–642 (2016).
- 32. Zheng, N. & Shabek, N. Ubiquitin Ligases: Structure, Function, and Regulation. *Annu Rev Biochem* **86**, 129–157 (2017).
- 33. Mattiroli, F. & Sixma, T. K. Lysine-targeting specificity in ubiquitin and ubiquitin-like modification pathways. *Nature Structural & Molecular Biology 2014 21:4* **21**, 308–316 (2014).
- 34. Deol, K. K., Lorenz, S. & Strieter, E. R. Enzymatic Logic of Ubiquitin Chain Assembly. *Front Physiol* **10**, 1–14 (2019).
- 35. Michel, M. A., Komander, D. & Elliott, P. R. Enzymatic assembly of ubiquitin chains. *Methods in Molecular Biology* **1844**, 73–84 (2018).
- 36. Blythe, E. E., Olson, K. C., Chau, V. & Deshaies, R. J. Ubiquitin- A nd ATP-dependent unfoldase activity of P97/VCP•NPLOC4•UFD1L is enhanced by a mutation that causes multisystem proteinopathy. *Proc Natl Acad Sci U S A* **114**, E4380–E4388 (2017).
- 37. Faggiano, S., Alfano, C. & Pastore, A. The missing links to link ubiquitin: Methods for the enzymatic production of polyubiquitin chains. *Anal Biochem* **492**, 82–90 (2016).
- 38. van der Schoot, J. M. S. *et al.* Functional diversification of hybridoma-produced antibodies by CRISPR/HDR genomic engineering. *Sci Adv* **5**, eaaw1822 (2019).

- 39. Luchansky, S. J., Lansbury, P. T. & Stein, R. L. Substrate recognition and catalysis by UCH-L1. *Biochemistry* **45**, 14717–14725 (2006).
- 40. Larsen, C. N., Krantz, B. A. & Wilkinson, K. D. Substrate specificity of deubiquitinating enzymes: Ubiquitin C-terminal hydrolases. *Biochemistry* **37**, 3358–3368 (1998).
- 41. Navarro, M. F., Carmody, L., Romo-Fewell, O., Lokensgard, M. E. & Love, J. J. Characterizing substrate selectivity of ubiquitin C-terminal hydrolase-L3 using engineered α -linked ubiquitin substrates. *Biochemistry* **53**, 8031–8042 (2014).
- 42. Gays, F. et al. The Mouse Tumor Cell Lines EL4 and RMA Display Mosaic Expression of NK-Related and Certain Other Surface Molecules and Appear to Have a Common Origin. *The Journal of Immunology* **164**, 5094–5102 (2000).
- 43. van Tilburg, G. B. A. *et al.* K27-Linked Diubiquitin Inhibits UCHL3 via an Unusual Kinetic Trap. *Cell Chem Biol* **28**, 191-201.e8 (2021).
- 44. Mevissen, T. E. T. *et al.* OTU deubiquitinases reveal mechanisms of linkage specificity and enable ubiquitin chain restriction analysis. *Cell* **154**, 169 (2013).
- 45. el Oualid, F. *et al.* Chemical synthesis of ubiquitin, ubiquitin-based probes, and diubiquitin. *Angewandte Chemie International Edition* **49**, 10149–10153 (2010).
- 46. Hameed, D. S., Sapmaz, A. & Ovaa, H. How Chemical Synthesis of Ubiquitin Conjugates Helps to Understand Ubiquitin Signal Transduction. *Bioconjug Chem* **28**, 805–815 (2017).
- 47. Huppelschoten, Y. & van der Heden van Noort, G. J. State of the art in (semi-) synthesis of Ubiquitin- and Ubiquitin-like tools. *Semin Cell Dev Biol* (2021) doi:10.1016/J. SEMCDB.2021.11.025.
- 48. Hospenthal, M. K., Freund, S. M. v & Komander, D. Assembly, analysis and architecture of atypical ubiquitin chains. doi:10.1038/nsmb.2547.
- 49. Jendroszek, A. & Kjaergaard, M. Nanoscale spatial dependence of avidity in an IgG1 antibody. *Scientific Reports 2021 11:1* **11**, 1–10 (2021).
- 50. Clague, M. J., Urbé, S. & Komander, D. Breaking the chains: deubiquitylating enzyme specificity begets function. *Nature Reviews Molecular Cell Biology 2019 20:6* **20**, 338–352 (2019).
- 51. Hingorani, S. R. *et al.* Trp53R172H and KrasG12D cooperate to promote chromosomal instability and widely metastatic pancreatic ductal adenocarcinoma in mice. *Cancer Cell* **7**, 469–483 (2005).
- 52. Benonisson, H. *et al.* CD3-Bispecific Antibody Therapy Turns Solid Tumors into Inflammatory Sites but Does Not Install Protective Memory. *Mol Cancer Ther* **18**, 312–322 (2019).
- 53. Ran, F. A. et al. Genome engineering using the CRISPR-Cas9 system. Nature

Protocols 2013 8:11 8, 2281-2308 (2013).

54. Geurink, P. P. *et al.* Development of Diubiquitin-Based FRET Probes To Quantify Ubiquitin Linkage Specificity of Deubiquitinating Enzymes. *ChemBioChem* **17**, 816–820 (2016).